EBioMedicine 31 (2018) 92–109

Contents lists available at ScienceDirect

EBioMedicine

journal homepage: www.ebiomedicine.com

Research Paper

Salmonella Typhi Colonization Provokes Extensive Transcriptional Changes Aimed at Evading Host Mucosal Immune Defense During Early Infection of Human Intestinal Tissue

K.P. Nickerson [a,b,**], S. Senger [a,b], Y. Zhang [c], R. Lima [a], S. Patel [a], L. Ingano [a], W.A. Flavahan [d], D.K.V. Kumar [e], C.M. Fraser [c], C.S. Faherty [a,b], M.B. Sztein [f], M. Fiorentino [a,b], A. Fasano [a,b,*]

[a] Department of Pediatric Gastroenterology, Mucosal Immunology and Biology Research Center, Massachusetts General Hospital, Boston, MA, United States
[b] Department of Pediatrics, Harvard Medical School, Harvard University, Boston, MA, United States
[c] Institute for Genome Sciences, University of Maryland School of Medicine, Baltimore, MD, United States
[d] Department of Pathology, Massachusetts General Hospital, Boston, MA, United States
[e] Department for the Neuroscience of Genetics and Aging, Massachusetts General Hospital, Boston, MA, United States
[f] Center for Vaccine Development, Department of Pediatrics, University of Maryland, Baltimore, MD, United States

ARTICLE INFO

Article history:
Received 1 November 2017
Received in revised form 2 April 2018
Accepted 5 April 2018
Available online 12 April 2018

Keywords:
Typhoid fever
Salmonella
Snapwell™ system
Human tissue
Terminal ileum
Immune system
Innate immunity
Immune evasion
Host-pathogen interaction
Vaccine development
Intestinal organoids
Organoid monolayer

ABSTRACT

Commensal microorganisms influence a variety of host functions in the gut, including immune response, glucose homeostasis, metabolic pathways and oxidative stress, among others. This study describes how *Salmonella* Typhi, the pathogen responsible for typhoid fever, uses similar strategies to escape immune defense responses and survive within its human host. To elucidate the early mechanisms of typhoid fever, we performed studies using healthy human intestinal tissue samples and "mini-guts," organoids grown from intestinal tissue taken from biopsy specimens. We analyzed gene expression changes in human intestinal specimens and bacterial cells both separately and after colonization. Our results showed mechanistic strategies that *S.* Typhi uses to rearrange the cellular machinery of the host cytoskeleton to successfully invade the intestinal epithelium, promote polarized cytokine release and evade immune system activation by downregulating genes involved in antigen sampling and presentation during infection. This work adds novel information regarding *S.* Typhi infection pathogenesis in humans, by replicating work shown in traditional cell models, and providing new data that can be applied to future vaccine development strategies.

1. Introduction

Bacterial pathogens represent a significant global burden to human health resulting in chronic infection, significant mortality, certain cancers, and diminished quality of life [23,38]. *Salmonella enterica* serovar Typhi (STY) is a human-restricted, gastrointestinal pathogen whose successful infection results in Typhoid fever or chronic infection [30]. Typhoid fever is frequently fatal when untreated in pediatric or immunocompromised populations [9,31,51,79]. It affects an estimated 11.9 to 26.9 million people annually [6,49,50], with estimated financial burdens equaling roughly a third of the gross national income for patients in undeveloped areas of Southeast Asia [35]. Current treatments depend on antibiotics; however, STY is rapidly developing antibiotic resistance, thereby increasing both the risk and severity of infection.

STY is a Gram-negative, enteric pathogen of the genus *Salmonellae*, species enterica, subspecies enterica. The subspecies enterica represents

Abbreviations: STY, Salmonella Typhi; STM, *Salmonella* Typhimurium; M cells, Microfold cells; CFU, colony forming units; LB, Luria Burtoni broth; DMEM, Dulbecco's Modified Eagle Medium; PBS, phosphate buffered saline; DTT, dithiothreitol; EDTA, ethylenediaminetetraacetic acid; ISC, intestinal stem cell; DAPT, N-[2S-(3,5-difluorophenyl)acetyl]-L-alanyl-2-phenyl-1,1-dimethylethyl ester-glycine; qPCR, quantitative reverse transcriptase polymerase chain reaction; FITC, fluorescein isothiocyanate; TEER, trans-epithelial electrical resistance; RNA, ribonucleic acid; LDH, lactate dehydrogenase; H&E, hematoxylin and eosin; PAS, periodic acid Schiff; TEM, transmission electron microscopy; IL, interleukin.

* Corresponding author at: A. Fasano, Center for Celiac Research, Mucosal Immunology and Biology Research Center, Massachusetts General Hospital East, Bldg 114, 16th St (Mail Stop 114-3503), Charlestown, MA 02129-4404, United States.
** Correspondence to: K.P. Nickerson, Mucosal Immunology and Biology Research Center, Massachusetts General Hospital East, Bldg 114, 16th St (Mail Stop 114-3503), Charlestown, MA 02129-4404, United States.
E-mail addresses: kpnickerson@mgh.harvard.edu (K.P. Nickerson), afasano@mgh.harvard.edu (A. Fasano).

https://doi.org/10.1016/j.ebiom.2018.04.005

two serovars: Typhimurium and Typhi. Genetically related, but phenotypically divergent, *S.* Typhimurium (STM) can cause localized inflammation of the small intestine, diarrhea and cramping. Conversely, STY infection has an incubation period of up to two weeks and results in systemic bacteremia with limited or no gastrointestinal symptoms. Comparative genomics between the two serovars reveals 480 STM-unique genes and 600-STY-unique genes [66]; notable STY genetic acquisitions include a capsule-encoding specific pathogenicity island (SPI)[78], two human-like serine-threonine kinases [73] and a typhoid toxin [18,21]. Numerous STY genes contain mutations relative to the STM homologs, with 0.6% of the STM genome encoding pseudogenes compared to 5% in the STY genome [66].

Current STY vaccination strategies include products that are expensive to produce and store. The attenuated oral vaccine Ty21a, which requires several immunizations to create a sustained immune response, confers protection in 62–96% of vaccinated individuals [41]. Alternative vaccine candidates currently in phase I and phase II studies have been generated by targeting virulence genes related to acid resistance, stress response, osmolarity and invasion. These gene targets are combined with gene deletions resulting in limited intracellular replication [24]. In most STY vaccine candidates, deleted genes attenuate infection. A notable exception is the constitutive expression of the STY-specific [82] immune-capsule suppressing regulator [78] *tviA* gene [24]. Despite the development of several vaccine strains against STY, no strategy confers long-term protection in a cost-effective manner.

Vaccine development against typhoid fever is hindered by significant assumptions about how *S.* Typhi causes infection in its human host. Specifically, no data are available regarding STY interaction with the small intestinal mucosa as the first step in the cascade of events ultimately leading to infection. Moreover, there have been no studies evaluating bacterial gene expression and consequences on host gene expression that occur during these critical early moments of infection. Despite fundamental differences in the pathology of infected humans relative to infected mice, and significant genomic differences between the two serovars, our current understanding of STY infection is mainly derived from the STM mouse model. Moreover, the two-week incubation period between STY exposure and onset of disease symptoms demonstrates a critical window in which STY infection is active prior to the onset of clinical disease. In recent years, human-derived organoid systems [19,64,67,80,84] or three-dimensional cell line models [29,60,68,69] have gained traction as a strategy to study host-pathogen interactions. These models have enabled new insight into cellular response during early STM infection to identify the role of bacterial genes n, such as the SPI-1 operon [60], or STM manipulation of signaling cascades [84]; however, few studies combining STY and human-derived organoid monolayers have been published.

Our work overcomes these shortfalls by placing STY bacteria directly onto human small intestinal tissue. In this study, we use an ex vivo, human intestinal tissue infection model and a human organoid-derived monolayer model. Infected biopsies were analyzed for transcriptional changes, cytokine profiling and electron microscopy, with specific mechanisms explored using the organoid monolayer model. This work sought to detail critical early events in Typhoid fever development to understand pathogenic mechanisms in human-derived tissue with the goal of identifying novel targets for vaccine development.

2. Materials and Methods

2.1. Bacterial Strains, Growth Conditions and Biopsy Infection

For all experiments, *Salmonella enterica* serovar Typhi strain Ty2 (STY, ATCC® Number: 700931) or serovar Typhimurium strain SL1344 (STM) (kind gift of Bobby Cherayil, Massachusetts General Hospital, Boston MA) were re-streaked bi-monthly on LB-agar plates. For experiments conducted under traditional laboratory conditions, an overnight culture from a single colony of STY or STM was prepared in Miller formula LB-broth (Sigma, St. Louis, MO) at 37 °C with shaking at 225 rpm. The next day, overnight cultures were diluted 1:50 into secondary subcultures and grown to log phase. To prepare the bacteria grown under pro-invasion conditions, a day culture in Miller formula LB broth from a single colony of STY or STM was started at 37 °C without shaking. After 4-8 h growth, a secondary culture diluted 1:50 in Miller LB was prepared and grown overnight at 37 °C without shaking. Bacteria were normalized to an OD600 of 0.5 prior to experimentation, pelleted by centrifugation and resuspended in warm Dulbecco's Modified Eagle Medium (DMEM) (Gibco, Grand Island, NY) for use in infection. All biopsies were infected with 1×10^8 bacteria in 250 μL DMEM for a maximum of 2 h. Biopsies were mounted using a snapwell system (Corning, Corning NY) with orientation confirmed by a dissecting microscope. Mounted biopsies acclimated for 30 m prior to removal of media and replacement with control DMEM or DMEM containing STY or SL1344. After 2 h of infection, apical and basolateral medium and biopsies were collected. For gentamicin protection assays, after 2 h infection the apical surface was washed 3× in phosphate buffered saline (PBS), and DMEM containing 5μg/mL gentamicin (Gibco) was added for 30 m at 37 °C. Afterward, biopsies were washed in PBS (Gibco) and subsequently homogenized in 0.5% Triton-X (Sigma) in PBS for serial dilution plating to determine CFU/mL recovery.

2.2. Isolation and Generation of Human Organoids; Preparation of Organoid-derived Epithelial Monolayers

The isolation and generation of human organoids was adapted from the protocol published by VanDussen et al. [76]. Briefly, human terminal ileum biopsies were processed in dithiothreitol (DTT) and ethylenediaminetetraacetic acid (EDTA) in PBS with penicillin/streptomycin (P/S, Gibco) to isolate the crypt fractions. This process was repeated 4–5 times; the fractions with the greatest number of crypts were pooled and resuspended in Matrigel (Corning, NY). Spheres were maintained in culture in 1:1 LWRN-conditioned medium and Intestinal Stem Cell (ISC) medium supplemented with Y-27632 (Sigma or Calbiochem, La Jolla, CA) and A-8301 (Sigma or Tocris, Minneapolis, MN). Spheres were fed every 2–3 days and split prior to differentiation. Undifferentiated cells were seeded onto transwell inserts and maintained in culture until monolayers formed. 48 h prior to experiment, monolayers were treated with apical N-[2S-(3,5-difluorophenyl)acetyl]-L-alanyl-2-phenyl-1,1-dimethylethyl ester-glycine (DAPT) (Calbiochem) to induce differentiation. Monolayers were assessed by quantitative reverse transcriptase polymerase chain reaction (qPCR) and confocal microscopy to identify markers for differentiated epithelial cells, as well as, Trans epithelial electrical resistance (TEER) and fluorescein isothiocyanate (FITC) dextran to determine barrier integrity.

2.3. Human Donors

All protocols for recruitment of human subjects and use of human terminal ileum biopsies were approved by Massachusetts General Hospital / Partners Healthcare IRB (Protocol 2014P002001). Prospective donors without chronic medical conditions who were scheduled to undergo a diagnostic colonoscopy were screened for good general health. Exclusion criteria included pregnancy, a known diagnosis of an autoimmune disorder or any chronic medical condition that would increase the risk from a gastrointestinal biopsy, and an inability or unwillingness to provide written informed consent. Donors signing informed consent contributed four to eight biopsies that were transported to the laboratory and used immediately to maximize tissue viability.

2.4. RNA Isolation and Transcriptomic Analysis

Following treatment (mock or infection) biopsies were immediately snap frozen on dry ice and stored at −80 until use. The control biopsy

group contains four samples, the infected biopsy group contains five samples and the bacteria control group contains four samples. Biopsy ribonucleic acid (RNA) was isolated in Trizol (Ambion, Carlsbad CA), using the Direct-Zol isolation kit (Zymo, Irvine, CA) following manufacturer's instructions. RNA from purified bacterial cultures was isolated using the RNAeasy kit (Qiagen, Waltham, MA) following manufacturer's instructions. Purified RNA was submitted to GENEWIZ (Frederick, MD) for RNA-sequencing, bacterial rRNA and human rRNA depletion, RNA library preparation (multiplexing and cluster generation) and sequencing on a 1x50bp SR, HiSeq 2500; rapid run flow cells were conducted by GENEWIZ. The reads generated for each RNA sample were analyzed using an Ergatis-based RNA-Seq analysis pipeline [59]. Quality control of the sequences was performed using FastQC (version 0.10.0) [3]. Human sequencing reads were aligned to the *Homo sapiens* reference genome GRCh38.78 using TopHat (version 2.1.1) [34]. Bacterial reads were aligned to *Salmonella enterica* serovar Typhi strain Ty2 genome (NCBI Reference Sequence: NC_004631.1) using Bowtie (version 0.12.9) [40]. The number of reads that aligned to the predicted coding regions were determined using HTSeq (version 0.4.7) [5]. Differential gene expression was analyzed using DESeq (version 1.5.24) [4] Full data sets were uploaded to Ingenuity Pathway (licensed to W. Flavahan), and differentially expressed genes were used to identify the pathways changed in infected samples. To identify differentially expressed STY genes, read files were uploaded into KBASE [7] and analyzed as follows: Samples were assigned to control or experimental samples to define a sample set for downstream analysis. The reads were then aligned using Bowtie2 to create an RNAseq alignment set. Transcripts were then assembled using StringTie, and differential expression was identified using CuffDiff. Further analysis was conducted to create expression matrices, heatmaps or cluster analysis. Differentially expressed genes were uploaded into KEGG to map bacterial pathways. Data is accessible in GEO under accession GSE113333.

2.5. Cytokine Analysis

Multiplex cytokine profiling was conducted using a 13plex human pro-inflammatory profiling kit in a Mesoscale Discovery System platform (Meso Scale Diagnostics, Rockville MD). Apical and basolateral samples from infected and control biopsies were assayed per manufacturer's instructions. Results were calculated to determine total volume of cytokine released. Statistical significance was determined by one-way ANOVA with Tukey post-test and represent an n of 15 controls, 10 STM and 10 STY infected. $^{*}p \le 0.05$, $^{**}p \le 0.005$, $^{***}p \le 0.0005$.

2.6. Western Blot Analysis

Snap-frozen biopsies were thawed in RIPA buffer (Sigma) + 2× protease inhibitors (Roche, Burlington NC) + 2× phosphatase inhibitors (Roche) on ice. Biopsies were homogenized using biomasher II tubes (Kimble, Vineland NJ) and protein concentration was quantified by protein assay (Biorad, Hercules, CA). 10 μg of protein were run on a 4–20% protein gel (Biorad) and transferred onto membrane (Biorad). Membranes were blocked in 5% BSA for 30 m followed by overnight incubation in the following antibodies: mouse anti-β-tubulin (RRID:AB_2715541), rabbit anti-pP44/42 MAPK (RRID:AB_2315112), rabbit anti-p-SAPK/JNK (RRID:AB_823588), rabbit anti-pP38 (RRID:AB_2139682), rabbit anti-pP65 (RRID:AB_331284) (all Cell Signaling Technologies, Danvers, MA). Densitometry was calculated as: $((\text{P-gene/area})/(\text{Actin/Area})_{\text{experimental}})/((\text{P-gene/area})/(\text{Actin/Area})_{\text{Media Control}})$. Significance was calculated by paired, two-tailed *t*-test, $^{*}p \le 0.05$.

2.7. Permeability and Cell Viability

Apical supernatants were assessed for lactate dehydrogenase (LDH) release using Promega Cytox Kit (Promega, Madison, WI) per manufacturer's instructions. To assess paracellular permeability, biopsies were monitored using a TEER apparatus (World Precision Instruments, Sarasota, FL). Alternatively, passage of 1μg/mL 4kD FITC Dextran was assessed by florescence in the basolateral medium using Biotek Synergy 2 and compared against serial dilutions of stock FITC dextran to generate a standard curve. No significance was determined by paired, two-tailed *t*-test.

2.8. Immunostaining and Microscopy Studies

For immunostaining, hematoxylin & eosin (H&E) and Periodic Acid Schiff (PAS) analysis, biopsies were fixed in 4% paraformaldehyde at room temperature for 30 m followed by storage in 70% ethanol until paraffin embedding. Sections were stained using the antibodies against the following proteins: mouse anti-Actin (RRID:AB_11004139, Invitrogen/Thermo-Fisher), rabbit anti-Zo1 (RRID:AB_2533938, Invitrogen), mouse anti-EPCaM (RRID:AB_10981962, Thermo Fisher, Waltham, MA), rabbit anti-rab5 (RRID:AB_823625, Cell Signaling Technologies), goat anti-Muc2 (RRID:AB_2146667, Santa Cruz Biotechnology, Dallas, TX), mouse anti-*Salmonella* (RRID:AB_1125358, BD Biosciences, San Jose, CA), rabbit-anti-*Salmonella* (RRID:AB_561201, Pierce/Thermo-Fisher), rabbit-anti-*Salmonella*-biotin conjugated (RRID:AB_1018415, Invitrogen/Thermo-Fisher) and mouse anti-tubulin (RRID:AB_2715541, Cell Signaling Technologies). Fluorescent, conjugated, secondary monoclonal antibodies were used for detection. For samples using streptavidin-biotin detection, avidin-biotin blocking was performed prior to staining (Life Technologies/Thermo-Fisher). Samples were imaged using a Nikon A1SiR confocal microscope.

For transmission electron microscopy (TEM) analysis, samples were fixed in 2%PFA/2.5% Glut in 0.1 M Sodium Cacodylate followed by mounting on grids and imaged using a transmission electron microscope (JEOL, Peabody, MA).

3. Results

3.1. Human Intestinal Biopsies Are Susceptible to STY Infection

STY colonize and invade the distal ileum of humans [20]. Terminal ileum biopsies obtained during clinically indicated colonoscopies were mounted in microsnapwell devices to allow polarized exposure to microorganisms from the luminal side [8] (see schematic in Fig. 1A and donor characteristics in Table 1). The biopsies were infected with 10^8 CFU of STY. The bacterial inoculum was prepared by growing STY under static conditions in LB-miller to maximize the expression of genes important in epithelial cell invasion [75] (Fig. 1B,**C**). After 2 h, invasion and biopsy status was assessed by transmission electron microscopy (TEM), hematoxylin and eosin (H&E) staining for light microscopy, Periodic acid Schiff (PAS) staining for light microscopy and gentamicin protection assay. Intracellular bacteria were detected by TEM, H&E and gentamicin protection assay **(**Fig. 1D–F**)**. Microvilli destruction and epithelial cell disorganization were observed at sites of bacterial invasion (Fig. 1F, 4B). No gross differences in H&E were observed (Fig. 1D), while minor differences in mucus staining was observed after infection by PAS staining.

3.2. Downregulation of Genes Involved in the Host Immune Response Is Observed Through Transcriptomic Analysis

We performed RNA-sequencing to determine differentially expressed genes in both STY and host cells **(**Fig. 2A**,** qPCR validation in Supplementary Fig. 1**)**. Gene expression profiles from non-infected control biopsies and STY-infected biopsies were compared to determine significantly upregulated ($p \le 0.05$ and >2-fold induction) and downregulated ($p \le 0.05$ and <0.5-fold reduction) genes. Similar gene expression changes were observed across samples or control groups with some anticipated

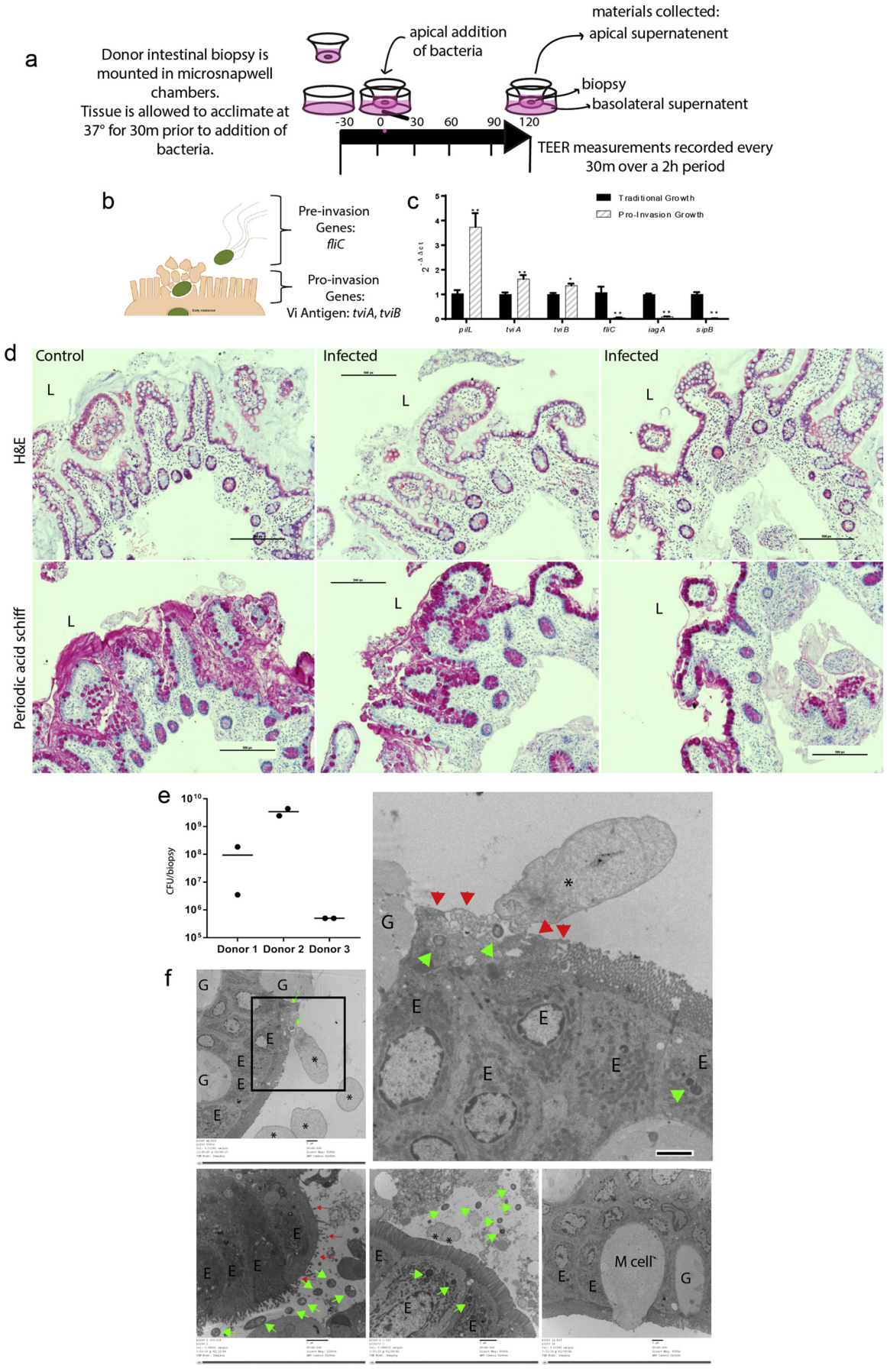
a
Donor intestinal biopsy is mounted in microsnapwell chambers.
Tissue is allowed to acclimate at 37° for 30m prior to addition of bacteria.
apical addition of bacteria
materials collected:
apical supernatenent
biopsy
basolateral supernatent
-30 0 30 60 90 120
TEER measurements recorded every 30m over a 2h period
b
Pre-invasion Genes: fliC
Pro-invasion Genes: Vi Antigen: tviA, tviB
c
Traditional Growth
Pro-Invasion Growth
2^-ΔΔct
pilL tviA tviB fliC iagA sipB
d
Control
Infected
Infected
H&E
Periodic acid schiff
L
e
CFU/biopsy
Donor 1 Donor 2 Donor 3
f
G
E
*
M cell

Table 1
Donor characteristics.

Study arm	Total recruited	Gender	Age	Race	Ethnicity
Microsnapwell infection	67	41 Males 26 Females	38 ± 31	2/67 Asian 2/67 AA or Black 6/67 Other 57/67 White	56/67 - Non-Hispanic or Latino 5/67 - Hispanic or Latino 6/67 - Declined or unknown
Organoid culture	8	3 Male 5 Female	6 (50–70) 2 (38–48)	8/8 White	1/8 Hispanic or Latino 7/8 Non-Hispanic or Latino

differences attributed to human-to-human variability (Fig. 2B). For human-specific genes, very few genes were upregulated in response to infection (Table 2A). Regulatory RNAs, the antioxidant *GSTM1*, zinc-interacting protein *CRIP1* and chemokine *CCL25* were among the eight significantly upregulated genes in infected samples. Reducing stringency to include genes that satisfied our significance cutoff but which were expressed below our 2-fold cutoff, revealed the expression of mucin *MUC5B,* the cytoskeletal gene *EPPK1* and several metabolism genes induced after infection. Conversely, 57 genes were significantly downregulated (Table 2B). Ultimately, the transcriptional profile of downregulated genes demonstrated significant clustering in several pathways including B-cell receptor signaling, coordination between innate and adaptive immune response, cell signaling and other pathways (Fig. 2C). This data set indicated that STY can hinder the activation of the mucosal immune response of the host during the first 2 h of invasion.

3.3. Invading STY Showed Differential Transcriptomic Profile Compared to Control Bacteria Related to Key Transcriptional and Invasive Pathways Important for Virulence

In general, pathogenic bacteria produce effector proteins that exploit host pathways to promote their survival. Therefore, we evaluated changes in bacterial gene expression occurring concurrently with the changes in host gene expression in the same tissue explants. Similar gene expression profiles were detected in control bacteria relative to the bacteria infecting the gut mucosa- with a single notable exception (Fig. 2D) -that was further emphasized during cluster analysis (Fig. 2E). To identify patterns in gene expression, clusters of genes with similar expression patterns were generated using KBASE (Fig. 2E), with the most significant groups showing similarity in gene expression changes for cluster 1: ribosome/metabolism genes; cluster 2: virulence genes and hypothetical proteins; and cluster 3: hypothetical proteins and unknown function. Surprisingly, the gene expression profile observed during STY infection (Fig. 2E, Table 3A and 3B) was remarkably different from what is predicted during STM infection (Fig. 2F). STM requires SPI-1 [1,32,75,85], *rpoS* and *ompR* [24] expression, which was observed in our bacterial inoculum and cultures grown in DMEM, but downregulated in bacteria invading the human gut mucosa. STY upregulated genes included numerous ribosome genes and enzymes. Upregulated enzymes (T1853, T0310, T4519 and T3866) encode eukaryotic-like serine/threonine kinases, acetyltransferases and inositol monophosphatase (Table 3A) which may have implications in the modulation of host signaling. Multiple components of the general secretory pathway (*secD*, *secF*, *secG*, secY) were also upregulated (Supplementary Fig. 1), suggesting that non-T3SS proteins are also utilized during infection. Several components of the SPI-2 operon including *sseB*, *sseA*, *ssaG*, *ssaM*, *ssaR*, *ssaS* and *ssaO* were downregulated relative to bacteria grown in DMEM alone (Table 3B, Supplementary Figs. 2, 2F), indicating that our model is capturing early events during *S.* Typhi pathogenesis, as expression of SPI-2 occurs during intracellular growth for STM. Interestingly, the SPI-7 operon-encoded Vi antigen is expressed in our inoculum with several genes located within the SPI-7 operon upregulated during biopsy infection (*tviD, tviE)*, consistent with previous reports generated by using bovine epithelial mucosa [62].

3.4. Cytokine Release Is Uncoupled from Transcriptional Replenishment and Mediated by Blocked MAPK and NF-kB Signaling Pathways

During clinical progression of typhoid fever [11,47,56,63,70], limited gastrointestinal symptoms are reported suggesting that STY invades with limited immune activation [82]. Using supernatants from infected biopsies, cytokine release was assayed using a multiplex ELISA method. Compared to control biopsies, infected biopsies demonstrated differential cytokine production both directionally (apically and basolaterally) and in response to infection with either STM or STY. The cytokine release profile was predominantly apical for STY and bidirectional for STM. For most cytokines, STM trigged a robust and uniform cytokine release, while STY infection led to mild cytokine release (e.g., IL-10, IL-2, IL-4) (Fig. 3A). Only half of the biopsies assayed secreted IL-13, IL-10, IL-4 and IL-2 in response to infection. The cytokine release profile for IFN-γ, IL-8, IL-1β and TNFα was more uniform across all donors. As much of the STY-induced cytokine release profile is skewed toward the apical pole, there was no significant increase in cytokine release on the basolateral pole. Significant basolateral release was observed with STM infection, both relative to control or STY-infected biopsies, demonstrating that the biopsies are viable and capable of responding to pathogen infection.

Despite significant cytokine release, no changes in cytokine transcripts were detected in the RNAseq data set (Fig. 2), suggesting that infection leads to cytokine release from stored intracellular pools and that bacterial exposure likely blocks transcription of new cytokines. The signaling cascades that lead to cytokine transcription are downstream of pattern recognition receptors' activation. Initiation of signaling cascades branching through MAPK and NF-κB were assayed by Western blot analysis of infected biopsies. After 60 min treatment in the microsnapwell chamber, phosphorylated p65, JNK, ERK and p38 was detected in all biopsies. A reduction in the phosphorylation state of p38, p65 and JNK was observed at 120 min post incubation for the control and STY infected samples, but remained phosphorylated in the STM infected biopsies (Fig. 3B). Analysis of our RNAseq data set predicted p38 (Fig. 3D) and NF-κB (Fig. 3E) to be important regulators of the gene expression changes observed during infection. The p38 MAPK regulation of numerous

Fig. 1. Modeling *S.* Typhi Infection: Human intestinal biopsies are susceptible to *Salmonella enterica* serovar Typhi infection. (A) A cartoon schematic detailing the microsnapwell model for infection of human intestinal biopsies. Biopsies are mounted between plastic inserts to preserve orientation by placing the basolateral surface down and the lumen-facing enterocytes in the apical opening. Biopsies are apically treated for 2 h (either media control, STY or STM). (B) An overview of known STY gene expression prior to and during early invasion. For reference: *fliC* is the major subunit of flagellin used prior to invasion to facilitate epithelial cell homing and Vi antigen genes *tviA* and *tviB* are expressed during invasion. (C) qPCR gene expression of STY bacteria in our pro-invasion inoculum relative to bacteria grown under traditional laboratory conditions. (D) Hematoxylin & Eosin and Periodic Acid Schiff images of fixed biopsies. Scale bars represent 500 pixels, "L" indicates the lumen. (E) Gentamicin protection assay showing the distribution of internalized STY across three donors. Invasion rates varied by donor, data presented represent counts for two separate biopsies from three distinct donors. Invasion rates for STM are 2–3× higher than STY (data not shown). (F)Invading and intracellular STY are observed by TEM, green arrows. Cytoskeletal rearrangements are denoted by *. Microvillus destruction is marked by red arrows. M cells are marked "M cell," enterocytes are labeled with "E," and goblet cells are marked with "G.' Scale bar is 2um for all TEM images.

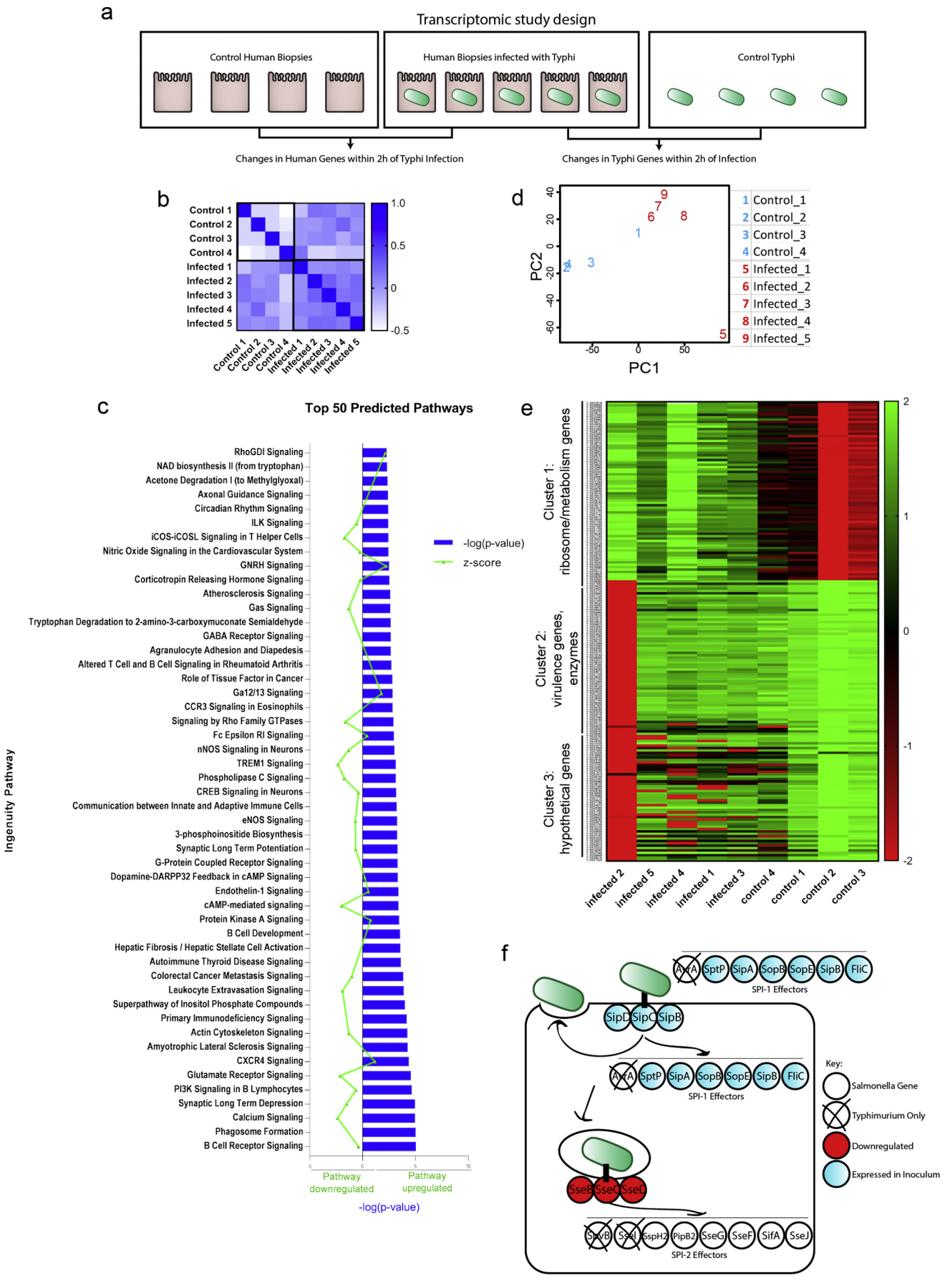
a
Transcriptomic study design
Control Human Biopsies
Human Biopsies infected with Typhi
Control Typhi
Changes in Human Genes within 2h of Typhi Infection
Changes in Typhi Genes within 2h of Infection
b
Control 1
Control 2
Control 3
Control 4
Infected 1
Infected 2
Infected 3
Infected 4
Infected 5
1.0
0.5
0
-0.5
d
PC2
PC1
1 Control_1
2 Control_2
3 Control_3
4 Control_4
5 Infected_1
6 Infected_2
7 Infected_3
8 Infected_4
9 Infected_5
c
Top 50 Predicted Pathways
Ingenuity Pathway
RhoGDI Signaling
NAD biosynthesis II (from tryptophan)
Acetone Degradation I (to Methylglyoxal)
Axonal Guidance Signaling
Circadian Rhythm Signaling
ILK Signaling
iCOS-iCOSL Signaling in T Helper Cells
Nitric Oxide Signaling in the Cardiovascular System
GNRH Signaling
Corticotropin Releasing Hormone Signaling
Atherosclerosis Signaling
Gas Signaling
Tryptophan Degradation to 2-amino-3-carboxymuconate Semialdehyde
GABA Receptor Signaling
Agranulocyte Adhesion and Diapedesis
Altered T Cell and B Cell Signaling in Rheumatoid Arthritis
Role of Tissue Factor in Cancer
Ga12/13 Signaling
CCR3 Signaling in Eosinophils
Signaling by Rho Family GTPases
Fc Epsilon RI Signaling
nNOS Signaling in Neurons
TREM1 Signaling
Phospholipase C Signaling
CREB Signaling in Neurons
Communication between Innate and Adaptive Immune Cells
eNOS Signaling
3-phosphoinositide Biosynthesis
Synaptic Long Term Potentiation
G-Protein Coupled Receptor Signaling
Dopamine-DARPP32 Feedback in cAMP Signaling
Endothelin-1 Signaling
cAMP-mediated signaling
Protein Kinase A Signaling
B Cell Development
Hepatic Fibrosis / Hepatic Stellate Cell Activation
Autoimmune Thyroid Disease Signaling
Colorectal Cancer Metastasis Signaling
Leukocyte Extravasation Signaling
Superpathway of Inositol Phosphate Compounds
Primary Immunodeficiency Signaling
Actin Cytoskeleton Signaling
Amyotrophic Lateral Sclerosis Signaling
CXCR4 Signaling
Glutamate Receptor Signaling
PI3K Signaling in B Lymphocytes
Synaptic Long Term Depression
Calcium Signaling
Phagosome Formation
B Cell Receptor Signaling
-log(p-value)
z-score
Pathway downregulated
Pathway upregulated
-log(p-value)
e
Cluster 1: ribosome/metabolism genes
Cluster 2: virulence genes, enzymes
Cluster 3: hypothetical genes
infected 2
infected 5
infected 4
infected 1
infected 3
control 4
control 1
control 2
control 3
f
SPI-1 Effectors
SPI-2 Effectors
Key:
Salmonella Gene
Typhimurium Only
Downregulated
Expressed in Inoculum

Table 2A
Human genes upregulated after 2 h infection with *S.* Typhi.

Feature.ID	p.Value	LFC infected/control	Gene name	Description (from uniprot)
Significant genes (P-value < 0.005 and log fold change (LFC) > 1.5)				
ENSG00000274519	3.88E-16	6.11	*mir3687–1*	Uncharacterized microRNA
ENSG00000231609	7.27E-08	2.96	*LOC100132215*	Uncharacterized locus
ENSG00000134184	5.53E-05	2.41	*GSTM1*	Conjugation of reduced glutathione to a wide number of exogenous and endogenous hydrophobic electrophiles.
ENSG00000185347	4.38E-12	1.91	*C14orf80*	Uncharacterized protein
ENSG00000237973	7.73E-09	1.86	*MTCO1P12*	Pseudogene
ENSG00000275783	8.85E-10	1.79	*MIR3648*	Uncharacterized microRNA
ENSG00000213145	6.81E-07	1.58	*CRIP1*	Seems to have a role in zinc absorption and may function as an intracellular zinc transport protein
ENSG00000131142	5.42E-09	1.56	*CCL25*	Potentially involved in T-cell development. Recombinant protein shows chemotactic activity on thymocytes, macrophages, THP-1 cells, and dendritic cells but is inactive on peripheral blood lymphocytes and neutrophils.
Significant genes (P-value > 0.005)				
ENSG00000117983	2.94E-08	1.46	*MUC5B*	Gel-forming mucin that is thought to contribute to the lubricating and viscoelastic properties of whole saliva and cervical mucus.
ENSG00000248527	5.12E-07	1.31	*MTATP6P1*	Pseudogene
ENSG00000198840	4.32E-05	1.29	*ND3*	Core subunit of the mitochondrial membrane respiratory chain NADH dehydrogenase
ENSG00000140323	3.12E-05	1.28	*DISP2*	Smoothened signaling pathway
ENSG00000216560	9.32E-06	1.23	*LINC00955*	Uncharacterized locus
ENSG00000212907	1.12E-05	1.2	*ND4L*	Core subunit of the mitochondrial membrane respiratory chain NADH dehydrogenase
ENSG00000228253	3.62E-06	1.19	*ATP8*	Mitochondrial membrane ATP synthase (F1F0 ATP synthase or Complex V) produces ATP from ADP in the presence of a proton gradient across the membrane which is generated by electron transport complexes of the respiratory chain.
ENSG00000206077	4.28E-05	1.19	*ZDHHC11B*	Protein-cysteine S-palmitoyltransferase activity
ENSG00000068078	7.80E-05	1.13	*FGFR3*	Tyrosine-protein kinase that acts as cell-surface receptor for fibroblast growth factors and plays an essential role in the regulation of cell proliferation, differentiation and apoptosis.
ENSG00000261150	5.71E-05	1.09	*EPPK1*	Cytoskeletal linker protein that connects to intermediate filaments and controls their reorganization in response to stress

immune functions (blue, Fig. 3D), with genes downregulated (red) or upregulated (green) after infection, is consistent with STY inhibition of these pathways to disarm the host innate and adaptive immune responses during early infection. These pathways have been identified as targets of *S.* Typhi in published literature demonstrating NF-κB inhibition in monocytes [74] or MAPK inhibition in the gallbladder epithelium [67].

3.5. STY Targets the Host Cytoskeleton to Infect the Intestinal Epithelium

Bacteria often manipulate the host cytoskeleton during invasion [14,25,43,52,61,72]. Within our RNAseq data set, genes involved in cytoskeletal reorganization were downregulated. Formation of cellular protrusions, cytoplasm organization, cytoskeleton reorganization and microtubule dynamics were all identified as pathways predicted to be affected by STY infection (Fig. 4A). TEM analysis revealed STY invading the intestinal mucosa via the apical surface of the enterocyte (Fig. 4B). Sites of bacterial invasion are accompanied by microvilli destruction and long protrusions of host cytoskeleton originating from enterocytes. While M cells were observed by TEM (Fig. 1F), no association of STY with M cells was observed. Furthermore, cytoskeletal projections observed in Fig. 4B were also observed in organoid-derived epithelial monolayers (Fig. 4H**),** suggesting that microvilli dissolution and remodeling of the host cytoplasm creates a surface suitable for invasion reproducible in both models.

Subsequently, immunostaining of the cytoskeletal protein actin and the related tight junction protein, zonula occludens-1 (ZO-1), showed actin projections into the lumen beyond the normal cellular structure, while no changes in ZO-1 localization was detected (Fig. 4C). Despite changes in the cytoskeleton, no changes in paracellular permeability were observed during this early phase of infection as measured by mucosa-to-serosa 4kD FITC-dextran flux (Fig. 4D) and TEER (Fig. 4E). Additionally, no significant increase in LDH release was detected, indicating that the tissue biopsies were not undergoing cell death in response to bacterial infection (Fig. 4F). To further explore the role of the cytoskeleton in STY invasion, human organoid-derived epithelial monolayers were treated with medium containing the actin-inhibitor cytochalasin D or the microtubule inhibitor nocodazole prior to infection with STY. Inhibitor treatment prevented STY invasion relative to untreated control monolayers (Fig. 4G). Lastly, TEM of infected organoid-derived epithelial monolayers recapitulated phenotypes observed in the infected biopsies including cytoskeleton rearrangement, microvilli destruction and vesicle-contained intracellular bacteria (Fig. 4H).

3.6. Intracellular Trafficking, Activation of Immune Pathways and the Human-restricted Nature of STY

In addition to manipulating the cytoskeleton for cell entry, bacterial exploitation of the structural proteins dictates how the vesicles mature,

Fig. 2. Downregulation of genes involved in the host immune response is observed through transcriptomic analysis. (A) A schematic overview of the transcriptomic study design using human biopsies. (B) Similarity matrix compares gene expression between samples to show that control and infected biopsies behaved like other control or infected biopsies without extensive variation. (C) Ingenuity Pathway analysis reveals clustering of genes in the top 50 predicted pathways; −log (p-value) is shown in blue; the z-score indicating pathway upregulation or downregulation is shown in green. (D) Principle components analysis shows that bacterial gene expression changes cluster based on infecting group or control group (C). (E) Bacterial genes clustered in three significant groups based on transcriptional changes. Cluster one encompasses genes required for gene expression; cluster two contains virulence genes, and cluster three contains a mix of hypothetical and virulence genes. (F) Comparison of genes utilized during STM infection overlaid with the gene expression profile of STY bacteria during invasion; it is important to note that genes expressed in our inoculum were not differentially expressed at 2 h invasion. SPI-1 effectors are important for facilitating invasion and are expressed early on; SPI-2 effectors are expressed later in infection and are important for intracellular survival. The SPI-2 genes *sseB, sseC, sseD* are downregulated at 2 h invasion of intestinal biopsies.

Table 2B
Human genes downregulated after 2 h Infection with *S.* Typhi.

Feature.ID	p.Value	LFC infected/control	Gene name	Function description (from uniprot)
Significant genes (P-value < 0.005 and log fold change (LFC) > 1.5)				
ENSG00000242512	3.15E-06	−4.03	*LINC01206*	Unknown
ENSG00000139304	5.61E-05	−3.87	*PTPRQ*	Dephosphorylates a broad range of phosphatidylinositol phosphates.
ENSG00000140798	4.56E-05	−3.67	*ABCC12*	Probable transporter.
ENSG00000172995	1.64E-05	−3.49	*ARPP21*	Calmodulin binding protein
ENSG00000280065	1.87E-11	−3.31		Unknown
ENSG00000081479	8.79E-08	−3.3	*LRP2*	Acts together with CUBN to mediate HDL endocytosis (By similarity).*
ENSG00000178568	1.65E-05	−3.21	*ERBB4*	Mediates phosphorylation of SHC1 and activation of the MAP kinases MAPK1/ERK2 and MAPK3/ERK1.
ENSG00000163554	7.66E-05	−3.2	*SPTA1*	Spectrin is the major constituent of the cytoskeletal network underlying the erythrocyte plasma membrane.*
ENSG00000140538	3.83E-10	−3.15	*NTRK3*	NTRK3 auto-phosphorylates and activates different signaling pathways, including the phosphatidylinositol 3-kinase/AKT and the MAPK pathways, that control cell survival and differentiation.
ENSG00000232111	4.22E-05	−3.13	*RP11-126O22.1*	Novel processed pseudogene
ENSG00000279003	2.15E-08	−3.09	*ENSG00000279003*	Unknown
ENSG00000263006	1.26E-05	−3.06	*ROCK1P1*	Transcribed unprocessed pseudogene
ENSG00000279185	1.51E-06	−3	*ENSG00000279185*	Unknown
ENSG00000181143	3.26E-14	−2.99	*MUC16*	Thought to provide a protective barrier against particles and infectious agents at mucosal surfaces
ENSG00000169436	4.07E-06	−2.91	*COL22A1*	Acts as a cell adhesion ligand for skin epithelial cells and fibroblasts.
ENSG00000140465	5.12E-06	−2.84	*CYP1A1*	Heme-thiolate monooxygenases.*
ENSG00000039139	2.86E-06	−2.83	*DNAH5*	Force generating protein of respiratory cilia. Produces force toward the minus ends of microtubules. Dynein has ATPase activity; the force-producing power stroke is thought to occur on release of ADP.
ENSG00000205592	5.15E-08	−2.83	*muc19*	May function in ocular mucus homeostasis.
ENSG00000148053	7.87E-08	−2.82	*NTRK2*	Receptor tyrosine kinase
ENSG00000279184	8.78E-11	−2.8	*RP3-323A16.1*	Unknown
ENSG00000007174	2.85E-07	−2.79	*DNAH9*	Force generating protein of respiratory cilia. Produces force toward the minus ends of microtubules.
ENSG00000166923	5.46E-12	−2.75	*GREM1*	Cytokine
ENSG00000186487	1.69E-05	−2.74	*MYT1L*	May function as a pan neural transcription factor associated with neuronal differentiation.
ENSG00000127241	5.72E-06	−2.74	*MASP1*	Functions in the lectin pathway of complement, which performs a key role in innate immunity by recognizing pathogens through patterns of sugar moieties and neutralizing them.
ENSG00000172724	1.09E-05	−2.73	*CCL19*	May play a role in inflammatory and immunological responses and in normal lymphocyte recirculation and homing. May play an important role in trafficking of T-cells in thymus, and T-cell and B-cell migration to secondary lymphoid organs. Binds to chemokine receptor CCR7.
ENSG00000137077	1.23E-13	−2.7	*CCL21*	Inhibits hemopoiesis and stimulates chemotaxis. Chemotactic in vitro for thymocytes and activated T-cells, but not for B-cells, macrophages, or neutrophils. Shows preferential activity toward naive T-cells. May play a role in mediating homing of lymphocytes to secondary lymphoid organs.
ENSG00000175820	1.38E-05	−2.69	*CCDC168*	Unknown
ENSG00000280156	8.84E-13	−2.69	*AC006548.28*	Unknown
ENSG00000168702	5.33E-05	−2.68	*LRP1B*	Potential cell surface proteins that bind and internalize ligands in the process of receptor-mediated endocytosis.
ENSG00000165323	9.60E-07	−2.65	*FAT3*	May play a role in the interactions between neurites derived from specific subsets of neurons during development.
ENSG00000101638	1.22E-05	−2.64	*ST8SIA5*	This protein is involved in the pathway protein glycosylation, which is part of protein modification.
ENSG00000089250	3.31E-05	−2.64	*NOS1*	Produces nitric oxide which is a messenger molecule with diverse functions throughout the body.
ENSG00000172023	1.92E-11	−2.54	*REG1B*	Uncharacterized protein
ENSG00000273079	2.60E-08	−2.51	*GRIN2B*	NMDA receptor subtype of glutamate-gated ion channels with high calcium permeability and voltage-dependent sensitivity to magnesium.

For the full list of downregulated genes, please see Supplementary Table 1.

migrate and target bacteria for clearance [71]. During early invasion, bacteria co-localized with tubulin (Fig. 5A) but they were not present in vesicles labeled with the early endosome protein Rab5. Intracellular bacteria contained within vesicles by TEM (Figs. 1F, 4B) were also observed, but the vesicle identity remains unclear. It is possible that Rab proteins are not present on these vesicles, as STM effector proteins target Rab proteins to block maturation of the autophagolysosome [13,28]. Our understanding of STY trafficking inside the epithelial cell is extremely limited. Furthermore, in our transcriptomic data set, we observe downregulation of several genes critical to bacterial clearance (including *CYBB* and *NOS)* in the mature phagosome (Fig. 5B). These data suggest that STY disarms the cellular machinery needed to kill intracellular bacteria by downregulating functional phagosome genes.

4. Discussion

Enteric pathogens continue to be a significant public health burden in both developed and developing countries [12,38,42,44]. STY remains an elusive vaccine target [24,41], which is partly due to critical gaps in knowledge regarding how STY causes disease. Some of these gaps are addressed for the first time in this manuscript.

4.1. STY Blocks the Immune Response during Infection

STY produces a polysaccharide capsule known as the Vi antigen, which is thought to protect the bacterial cell from detection by pattern recognition receptors [33,75,81,82]. We conclude that STY further blocks activation of the innate immune system based on depressed or uninduced gene transcription, impaired signal transduction and apical cytokine release observed during human biopsy infection. STY expression of the Vi antigen during human infection (which includes the upregulated genes *vexD, vexB, tviE,* and *tviD*) is well-documented [82], and it masks lipopolysaccharide, peptidoglycan and flagellin from the host pattern recognition receptors. Several additional expressed STY genes that may also block innate immune activation by targeting signal transduction intermediates include the γ-proteobacteria conserved *suhB* gene [54], which encodes an inositol monophosphatase and functions in the modulation of inositol signaling [48].

Table 3A
Select *S.* Typhi genes upregulated after 2 h infection.

pGene	Gene	Log fold change	q-Value	Function
T_RS16275	t3210	3.72	0.0004	Preprotein translocase subunit SecG
T_RS09445	t1853	3.43	0.0004	Beta-hydroxydecanoyl-ACP dehydratase
T_RS18075	t3559	3.38	0.0004	Repressor of the Cpx envelope stress response pathway.
T_RS24905	T_RS24905	3.38	0.0004	Hypothetical protein
T_RS20765	t4085	3.35	0.0004	Preprotein translocase subunit SecY
T_RS24820	T_RS24820	3.22	0.0004	Hypothetical protein
T_RS24855	T_RS24855	3.16	0.0004	Hypothetical protein
T_RS04520	t0882	3.13	0.0004	Cold-shock protein CspJ
T_RS23945	T_RS23945	3.1	0.0004	Hypothetical protein
T_RS24535	T_RS24535	3.02	0.0004	Hypothetical protein
T_RS20790	t4090	2.97	0.0004	DNA-directed RNA polymerase subunit alpha
T_RS22875	t4496	2.93	0.0021	Pyrbi operon leader peptide
T_RS19685	t3869	2.83	0.0004	Hypothetical protein
T_RS23875	T_RS23875	2.71	0.0004	Hypothetical protein
T_RS01565	t0310	2.71	0.0004	Inositol monophosphatase
T_RS03930	t0780	2.7	0.0004	Glucose-1-phosphate cytidylyltransferase
T_RS19190	t3772	2.67	0.0004	Xanthine permease
T_RS03270	t0646	2.6	0.0039	Membrane protein
T_RS03285	t0650	2.59	0.0004	Phosphoenolpyruvate dependent, sugar transporting phosphotransferase system.
T_RS03290	t0649	2.59	0.0004	Phosphofructokinase
T_RS02365	t0466	2.58	0.0004	Acyltransferase
T_RS10080	T_RS10080	2.57	0.0011	Hypothetical protein
T_RS10085	t1980	2.57	0.0011	Translation initiation factor IF-1
T_RS08805	t1730	2.56	0.0004	Hypothetical protein
T_RS22990	t4521	2.53	0.0004	Hypothetical protein
T_RS22995	t4519	2.53	0.0004	Serine/threonine protein kinase
T_RS23000	t4520	2.53	0.0004	Serine/threonine protein kinase
T_RS19345	t3803	2.53	0.0004	LPS core heptose(II) kinase RfaY
T_RS05655	t1106	2.49	0.0004	Hypothetical protein
T_RS02155	T_RS02155	2.48	0.0004	
T_RS08555	t1680	2.46	0.0016	Sodium potassium/proton antiporter ChaA
T_RS03960	t0786	2.44	0.0004	Glycosyl transferase
T_RS08780	t1725	2.44	0.0004	Beta-ketoacyl-ACP reductase
T_RS02535	t0501	2.43	0.0004	Colicin V production protein
T_RS20635	t4059	2.42	0.0004	Elongation factor G
T_RS03925	t0779	2.39	0.0004	CDP-6-deoxy-delta-3,4-glucoseen reductase
T_RS14115	t2782	2.39	0.0004	Hypothetical protein
T_RS16300	t3215	2.38	0.0004	RNA binding protein found associated to pre-50S subunit of the ribosome.*
T_RS22250	t4371	2.38	0.0004	Integrase
T_RS03965	t0787	2.37	0.0004	Glycosyl transferase
T_RS22890	t4499	2.36	0.0004	Ornithine carbamoyltransferase
T_RS12270	t2413	2.36	0.0004	Trigger factor
T_RS08595	t1688	2.35	0.0004	Adenylosuccinate lyase
T_RS21345	t4196	2.34	0.0004	Hypothetical protein
T_RS00790	t0157	2.34	0.0004	Pyruvate dehydrogenase complex repressor
T_RS17570	t3461	2.31	0.0004	DNA-binding protein HU-alpha
T_RS16745	t3300	2.31	0.0004	Fis family transcriptional regulator
T_RS12085	t2377	2.31	0.0004	Adenine phosphoribosyltransferase
T_RS00330	t0067	2.3	0.0004	Carbamoyl-phosphate synthase small subunit
T_RS00865	t0172	2.29	0.0004	Hypothetical protein
T_RS03955	t0785	2.27	0.0004	Transporter
T_RS16250	t3205	2.27	0.0004	Transcription termination protein NusA
T_RS03175	t0627	2.26	0.0004	Hypothetical protein
T_RS14120	t2783 (iacP)	2.23	0.0004	Acyl carrier protein
T_RS12185	t2397	2.22	0.0004	Nitrogen regulatory protein P-II 2
T_RS03945	t0784	2.21	0.0004	CDP-paratose 2-epimerase
T_RS03950	t0783	2.21	0.0004	CDP-paratose synthase
T_RS19320	t3798	2.21	0.0004	Hypothetical protein
T_RS19325	t3799	2.21	0.0004	Hypothetical protein
T_RS03940	t0782	2.18	0.0004	LPS biosynthesis protein
T_RS09545	t1875	1.62	0.0067	Hypothetical protein
T_RS00205	t0042	1.61	0.0004	Transcriptional activator NhaR
T_RS22130	t4347	1.57	0.0004	Vi polysaccharide export inner-membrane protein VexB
T_RS22140	t4350	1.56	0.0037	Vi polysaccharide biosynthesis protein TviD
T_RS22145	t4349	1.56	0.0037	Vi polysaccharide biosynthesis protein TviE

For the full list of upregulated STY genes, please see Supplementary Table 2.

Legionella manipulates inositol signaling to enable creation of the *Legionella*-containing vacuole for survival [26]. Likewise, STM replicates within the *Salmonella*-containing vesicle (SCV). Generation of the SCV is dependent on the SPI-1 effectors SopB and SopE/E2[27], which modulate inositol signaling and Rab proteins, respectively. The *suhB* gene overcomes the rate-limiting step in inositol signaling to affect second messenger signaling, autophagy and cell death pathways [26]. Two additional upregulated STY specific-enzymes encode eukaryotic-like serine-threonine kinases (T4519, T4520). In data derived from the infection of immortalized macrophage cell lines, T4519 is required for both intracellular survival and IL-6 and TNF-α production, as well as for NFkB phosphorylation [73]. In line with our data, impaired activation

Table 3B
Select *S.* Typhi genes downregulated after 2 h Infection.

Locus	Gene	Log fold change	q-Value	Function
T_RS05760	t1128	−4.6998	0.000303	Heat-shock protein
T_RS20010	t3935	−4.68863	0.0047827	Membrane protein
T_RS16050	t3164	−4.42922	0.0356647	Serine/threonine dehydratase
T_RS06575,	t1288	−4.05222	0.0017506	Type III secretion system protein SsaS
T_RS15430	t3045	−3.931	0.0361737	Hypothetical protein
T_RS14420	t2844	−3.85909	0.0022412	Type I-E CRISPR-associated protein Cse1/CasA
T_RS09110	t1790	−3.82746	0.0267944	*N*-acetylneuraminate epimerase
T_RS01550	t0307	−3.74357	0.003615	Anaerobic sulfite reductase subunit B
T_RS18320	t3606	−3.66574	0.0054552	Hypothetical protein
T_RS00180	t0037	−3.62981	0.0033564	Sulfatase
T_RS23565	t4633	−3.62105	0.0106418	Fimbrial chaperone protein
T_RS15480	t3054	−3.57317	0.0234569	Amidohydrolase
T_RS07840	t1540	−3.5345	0.0046498	Membrane protein
T_RS20210	t3974	−3.52218	0.0198834	Ribokinase
T_RS09100	t1788	−3.50146	0.0095141	MFS transporter
T_RS05770	t1130	−3.4989	0.0031178	Hypothetical protein
T_RS11895	t2339	−3.48786	0.0253715	Allantoin permease
T_RS06445	t1262	−3.42977	7.20E-05	EscC/YscC/HrcC family type III secretion system outer membrane ring protein
T_RS06380	t1249	−3.42	0.0464325	Hypothetical protein
T_RS02200	t0435	−3.39407	0.0292125	Purine-nucleoside phosphorylase
T_RS06525	t1278	−3.383	2.18E-06	Pathogenicity island protein
T_RS09630	t1891	−3.37E+00	0.0149459	Hypothetical protein
T_RS06460	t1265	−3.36098	0.0492594	Chaperone for SseB and SseD
T_RS01555	t0308	−3.33498	0.0106668	Sulfite reductase subunit alpha
T_RS13295	t2616	−3.30635	0.0073327	Chaperone protein ClpB
T_RS06385	t1250	−3.30289	0.0493247	Pseudo hypothetical protein, frameshifted
T_RS02205	t0436	−3.2902	0.016477	Xanthosine permease
T_RS06035	t1180	−3.2816	0.0254963	Pyrimidine (deoxy)nucleoside triphosphate pyrophosphohydrolase
T_RS06540	t1281	−3.26407	5.89E-05	Type III secretion system protein SsaM,
T_RS14505	t2860	−3.26E+00	0.0025029	Fimbrial protein SteE
lpfA	t3659	−3.25935	0.0271651	Fimbrial protein
T_RS00190	t0039	−3.25E+00	0.0180323	Hypothetical protein
T_RS23005	t4522	−3.09E+00	0.0466588	Polarity suppression protein
modA,modB	t2105	−3.06609	0.0034703	Part of ModCBA molybdate transporter
T_RS13735	t2702	−3.05094	0.0136309	NrdH-redoxin
T_RS20205	t3973	−3.05052	0.0497433	Hypothetical protein
T_RS11900	t2340	−2.99758	0.03144	MFS transporter
T_RS06580,	t1289	−2.95076	0.0011772	Type III secretion system protein SsaT
T_RS06555	t1284	−2.91116	7.20E-05	SSaO Salmonella pathogenicity island 2 protein
T_RS16100	t3175	−2.83436	0.0014239	PTS galactitol/fructose transporter subunit II
T_RS09515	t1868	−2.80141	7.14E-05	Hypothetical protein
T_RS15520	t3062	−2.79169	0.002574	Molybdenum ABC transporter substrate-binding protein
T_RS16110	t3177	−2.77916	0.0346406	D-tagatose-bisphosphate aldolase, class II, non-catalytic subunit
T_RS21165	t4162	−2.7735	7.20E-05	Hypothetical protein
T_RS19870	t3906	−2.77198	0.0376913	Cyclic-guanylate-specific phosphodiesterase
T_RS01545	t0306	−2.76366	0.0243692	Sulfite reductase subunit C
T_RS23560	t4632	−2.75952	0.0347524	Frameshifted
T_RS06505	t1274	−2.73865	0.0360844	Type III secretion system needle protein SsaG
T_RS19490	t3831	−2.71975	0.0499517	Hypothetical protein
T_RS16450	t3244	−2.68263	0.011345	Glutamine amidotransferase
T_RS02280	t0450	−2.67886	0.0466588	Hypothetical protein
T_RS09750	t1914	−2.67E+00	0.0006626	Methyltransferase
T_RS23210	t4563	−2.66886	0.0212746	Membrane protein
T_RS23145	t4550	−2.6688	0.0477512	SAM-dependent methyltransferase
T_RS08510	t1671	−2.64519	0.0003457	Nitrate reductase molybdenum cofactor assembly chaperone
T_RS06895	t1352	−2.6331	0.0101017	Tail fiber protein
T_RS14890	t2935	−2.6154	0.0110453	Transcriptional regulator
T_RS04790	t0937	−2.59229	0.0423495	Cell wall hydrolase
T_RS18330	t3608	−2.58732	0.0054552	Hypothetical protein
T_RS07830	t1538	−2.56658	0.0114123	ABC transporter ATP-binding protein
T_RS18345	t3610	−2.48E+00	0.000754	Coproporphyrinogen III oxidase
sseA	t1265	−2.39E+00	0.0404711	Type III secretion system chaperone SseA
T_RS12810	t2522	−2.27364	0.0137239	Fimbrial chaperone protein
T_RS06465	t1266	−2.27192	0.0169695	SSeB necessary for the correct localization of SseC and SseD on the bacterial cell surface

For the full list of downregulated STY genes, please see Supplementary Table 3.

Fig. 3. Tissue response to *S.* Typhi infection reflects differential apical cytokine release. (A) Multiplexed ELISA analysis of pro-inflammatory and regulatory cytokines in control biopsies, STM or STY treated (black, red, blue, respectively). (B) As cytokine release is observed but no transcriptional upregulation is detected (per RNA-seq data set), intracellular signal transduction was assessed by western blot analysis to determine the phosphorylation state of NF-kB and MAPK from samples mounted in the microsnapwell system after exposure to media, STM or STY at time points of 60 min and 120 min. (C) Densitometry analysis of signaling blots. (D) Pathway analysis demonstrates a central role for MAPK in regulated cellular processes and gene expression important in development of immune responses. Note: All genes shown here are downregulated and their expression patterns predict inhibition of cell recruitment. (E) NF-kB is a central regulator of gene expression; its activation is critical to expression of genes downregulated in our RNAseq data set.

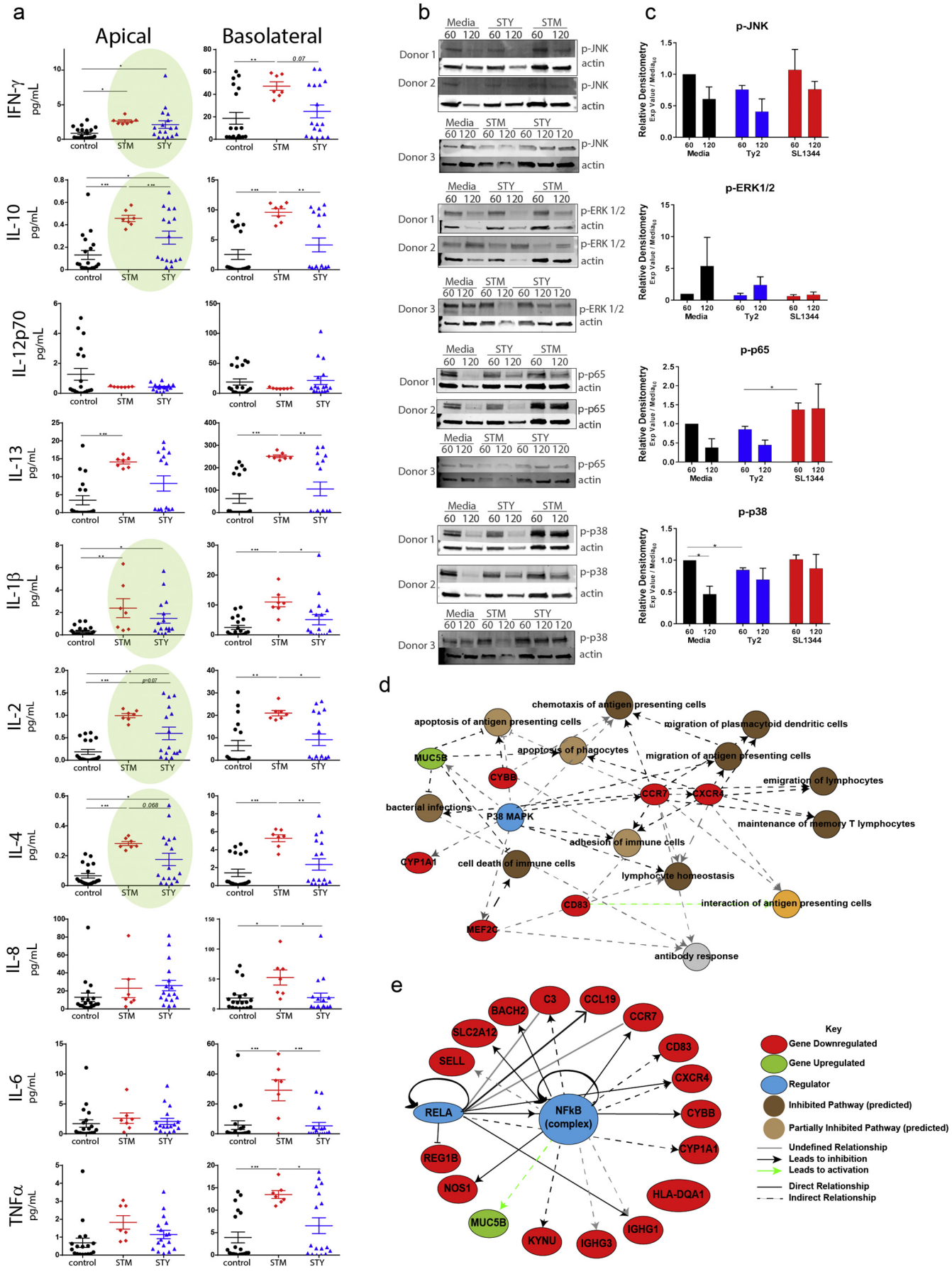
a
Apical
Basolateral
IFN-γ pg/mL
IL-10 pg/mL
IL-12p70 pg/mL
IL-13 pg/mL
IL-1β pg/mL
IL-2 pg/mL
IL-4 pg/mL
IL-8 pg/mL
IL-6 pg/mL
TNFα pg/mL
control
STM
STY
b
Media
STY
STM
60 120
Donor 1
Donor 2
Donor 3
p-JNK
p-ERK 1/2
p-p65
p-p38
actin
c
p-JNK
p-ERK1/2
p-p65
p-p38
Relative Densitometry
Exp Value / Media60
Media
Ty2
SL1344
d
chemotaxis of antigen presenting cells
apoptosis of antigen presenting cells
migration of plasmacytoid dendritic cells
apoptosis of phagocytes
migration of antigen presenting cells
MUC5B
CYBB
emigration of lymphocytes
CCR7
CXCR4
bacterial infections
P38 MAPK
maintenance of memory T lymphocytes
adhesion of immune cells
CYP1A1
cell death of immune cells
lymphocyte homeostasis
CD83
interaction of antigen presenting cells
MEF2C
antibody response
e
BACH2
C3
CCL19
CCR7
SLC2A12
CD83
SELL
CXCR4
RELA
NFkB (complex)
CYBB
CYP1A1
REG1B
NOS1
HLA-DQA1
MUC5B
KYNU
IGHG3
IGHG1
Key
Gene Downregulated
Gene Upregulated
Regulator
Inhibited Pathway (predicted)
Partially Inhibited Pathway (predicted)
Undefined Relationship
Leads to inhibition
Leads to activation
Direct Relationship
Indirect Relationship

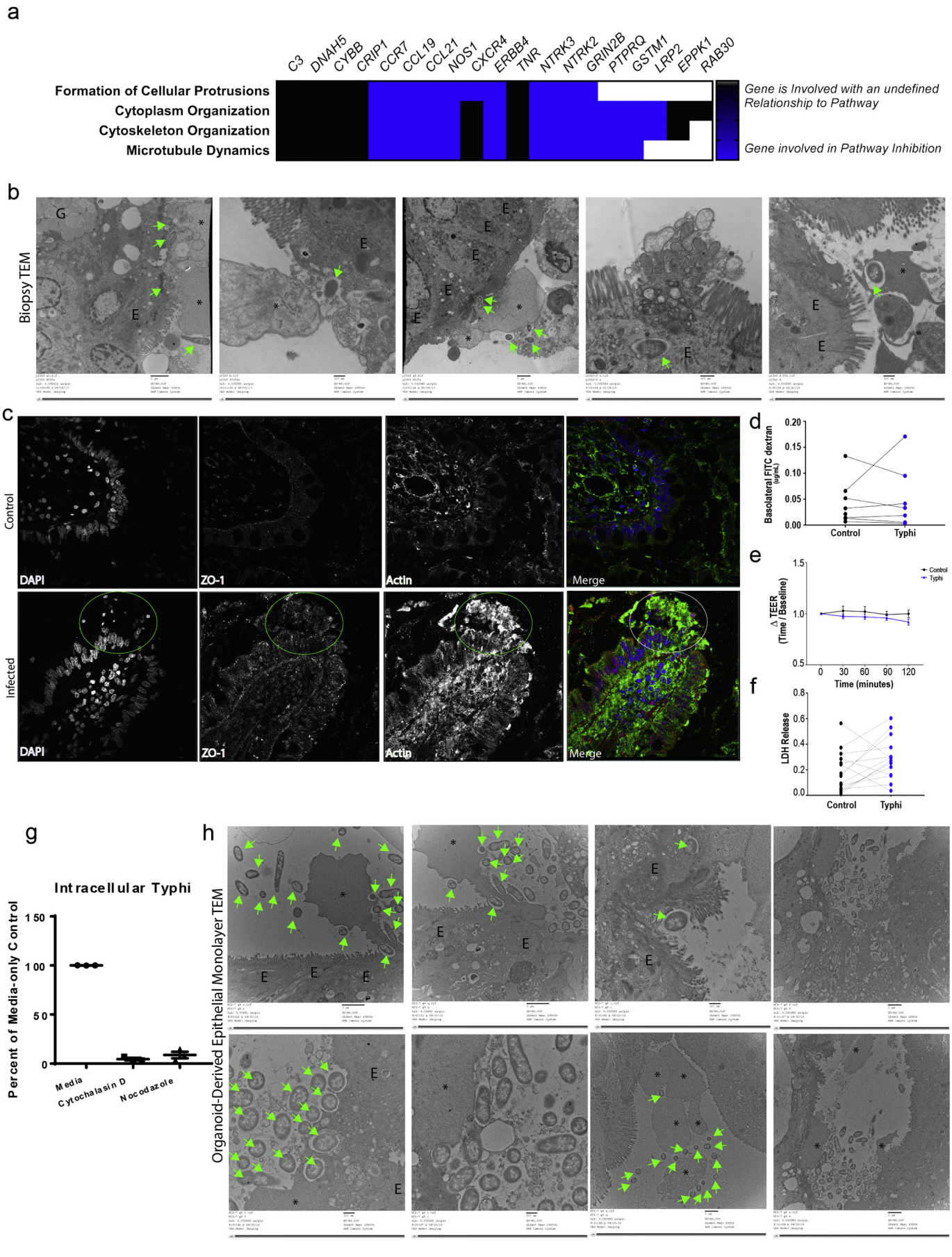
a
C3
DNAH5
CYBB
CRIP1
CCR7
CCL19
CCL21
NOS1
CXCR4
ERBB4
TNR
NTRK3
NTRK2
GRIN2B
PTPRQ
GSTM1
LRP2
EPPK1
RAB30
Formation of Cellular Protrusions
Cytoplasm Organization
Cytoskeleton Organization
Microtubule Dynamics
Gene is Involved with an undefined Relationship to Pathway
Gene involved in Pathway Inhibition
b
Biopsy TEM
c
Control
Infected
DAPI
ZO-1
Actin
Merge
d
Basolateral FITC dextran (ug/mL)
Control
Typhi
e
Δ TEER (Time / Baseline)
Time (minutes)
f
LDH Release
g
Intracellular Typhi
Percent of Media-only Control
Media
Cytochalasin D
Nocodazole
h
Organoid-Derived Epithelial Monolayer TEM

of signal transduction pathways not only prevents gene transcription changes and overall immune response development, but also blocks vesicular trafficking. *Salmonella*-mediated impaired vesicle maturation prevents lysosomal or autophagolysosomal bacterial killing [28,57], thereby allowing bacterial survival and preventing bacterial antigens to stimulate the class I/II major histocompatibility complex (MHC) antigen presentation pathways for the generation of adaptive immune responses. Combined, our data suggest that STY evade innate and adaptive immune responses through multiple and complementary approaches that begin immediately upon invasion and are actively regulated through secreted factors delivered to host enterocytes or the intestinal lumen.

Furthermore, in our model, major MHC-II and reactive oxygen species genes (NADPH-oxidase genes and nitric oxide synthase NOS) are transcriptionally downregulated in response to infection, which may further prevent the host response to STY. Additionally, important immune system genes are downregulated, indicating critical breakpoints in B-cell and T-cell maturation, activation and overall lymphoid cell recruitment to the sites of infection (Supplementary Figs. 3, 4). Our data, which support clinical observations that STY exposure fails to provoke an immune response, also identifies bacterial genes expressed in the modulation of the host immune response. Further studies and deletion constructs are pivotal to understand the function of these enzymes during STY infection. Our findings provide novel information on mechanisms responsible for the host cell's inability to kill STY. These mechanisms are linked to the inhibition of pathways preventing antigen recognition and, ultimately, the development of an adaptive immune response. This concept is supported by our pathway analysis showing differentially expressed genes associated with the deactivation of pathways involved in the crosstalk between innate and adaptive immune responses (Fig. 5C, Supplementary Fig. 3), B-cell receptor signaling (Supplementary Fig. 4) and the maturation of dendritic cells. Ultimately, the downregulation of cell surface genes such as *CD22*, *CD79A* and *IgG*, as well as intracellular signaling genes *PI3K* and transcription factor *PAX5*, underscores an inability of the STY infected host cell to activate the adaptive immune system, providing insight into how STY escape clearance by circumventing the host immune system activation.

4.2. STY Infects Enterocytes

Historically, enteric pathogens are thought to enter the host by crossing the gastrointestinal epithelium via specialized M-cells [16,17,46]. Through TEM analysis, we found numerous epithelial cells in various states of STY invasion. Although research supports a role for M-cells in STM infection [17], and to a lesser extent in STY infection [24], we observed that STY infection was predominantly via enterocytes in both tissue explants and gut organoid-derived monolayers, although previous studies have described mechanisms for apical invasion of enterocytes for STM [2]. Common themes observed in infected cells included microvilli destruction and cytoskeletal rearrangement affectingboth actin and tubulin. Furthermore, cytoskeletal projections created a site of invasion that seemed to recruit other STY bacterial cells to enter at the same location. We hypothesize that quorum sensing (QS) facilitates invasion in an energetically favorable manner, by which initial invading bacteria promote microvilli destruction and cytoskeletal rearrangement, and perhaps the release of QS molecules, resulting in cooperative invasion at the same site. STY produces QS molecules homologous to QseBC [53]; a communication system required for enterohemorrhagic *E. coli* pathogenesis [58]. Therefore, we hypothesize that the community of invading STY works together to suppress the immune activation in the same cell, enriching its chances of survival by creating invasion "hot spots." The conserved QS genes in the *qse* and *lux*/*lsr* operon are expressed in both our inoculum and invading bacteria, but not differentially expressed during invasion. Curiously, homologs of peptide-based QS genes are differentially expressed during invasion. Peptide-initiated QS is frequently observed in Gram-positive bacteria [65,77] but only the 'extracellular death factor' peptide QS signaling pathway has been described in Gram-negative *E. coli* [36,37,39]. QS molecules are produced in response to population density and to regulate virulence factors [45,65]. It is well-documented that QS molecules induce expression of SPI-1 in STM to promote invasion [15,22,53,55]. Importantly, pathogenesis of enterohemorrhagic *E. coli* depends on host and commensal derived QS molecules to initiate colon invasion, whereas the invasion stimulus for STY, and the potential role for QS, remains an area warranting future investigation.

4.3. Host-Specificity of Infection: STM vs. STY

STM causes infection in a genetically susceptible, antibiotic-treated mouse [10]. Hallmarks of infection include edema, neutrophil recruitment and bacterial infiltration of the liver, lymph nodes, spleen and cecum [10]. As STM can cause systemic infection, it is used as a model for STY infection in humans. When mice are exposed to STY, the resulting infection is self-limiting within the GI tract and shares very few clinical and pathogenic traits with human disease. Conversely, human infection with STM bacteria results in local gastrointestinal infection that resolves within a few days. Genetically, the two serovars are nearly identical; however STY has gained additional virulence genes [66,83] (notably, SPI-7) and is thought to have significantly fewer protein-coding genes than STM due to insertion sequences, truncations and mutations [66]. Despite genetic similarities, we observed extensive and divergent phenotypes with human infection by STY as compared to STM. As such, we noticed that the host genes upregulated during STY infection were nearly all divergent between human and mice. For example, the cytokine *CCL25* and the mitochondrial enzyme *ATP8* are both found in humans but not in mice (Table 4). Other genes, like the cytoskeletal remodeling gene *EPPK1*, shares only 75.5% protein identity with its mouse homologue, which allows us to speculate that some of the host specificity of infection is a direct extension of the genes upregulated during infection. Other variables are important here: e.g., human *MUC2* shares only 76% identity with its mouse homologue and the MUC2 product functions as a barrier protecting the intestinal epithelium from bacteria. As mice and humans have different pathogen susceptibility and crossing the mucus barrier is a significant challenge to infection, it would be interesting to study if the protein homology differences contribute to infection susceptibility. Further studies are required to evaluate the relative importance of each of the affected genes and virulence factors during the initial stages of infection.

Current vaccine candidates target the following genes in *S.* Typhi: *rpoS*, *galE*, *galK*, *ilvD*, *vexD*, *phoP*, *phoQ*, *aroC*, *ssaV*, *aroD*, *htrA* and *tviA*.

Fig. 4. Host response to Typhi infection: barrier function and antigen trafficking. (A) Differentially expressed genes cluster in cytoskeletal modulation pathways. Genes with an unidentified relationship to the pathway are shown in black; genes involved in pathway inhibition are shown in blue. (B, H) Reorganization of the cytoskeletal is observed upon STY association with intestinal biopsies and organoid-derived epithelial monolayers (H). Large scale bars are 2 μm, small scale bars are 500 nm. (C) Cellular protrusions are actin-dense as observed by immunostaining (C, circled). (D–F) No changes in paracellular permeability (D, E) are observed at early time points during infection supporting the fact that STY directly infected enterocytes of the intestinal epithelium, and that biopsy invasion is not accompanied by cell death (F). (G) Inhibition of the cytoskeleton using the actin inhibitor cytochalasin D or microtubule inhibitor nocodazole block STY entry into organoid-derived epithelial monolayers. (H) STY bacteria interact with the epithelium by promoting cytoskeletal rearrangement and internalization into vesicles like those observed in the infected biopsies. Invading and intracellular STY are observed by TEM, green arrows. Cytoskeletal rearrangements are denoted by * and enterocytes are labeled with "E." Large scale bars are 2 μm, small scale bars are 500 nm.

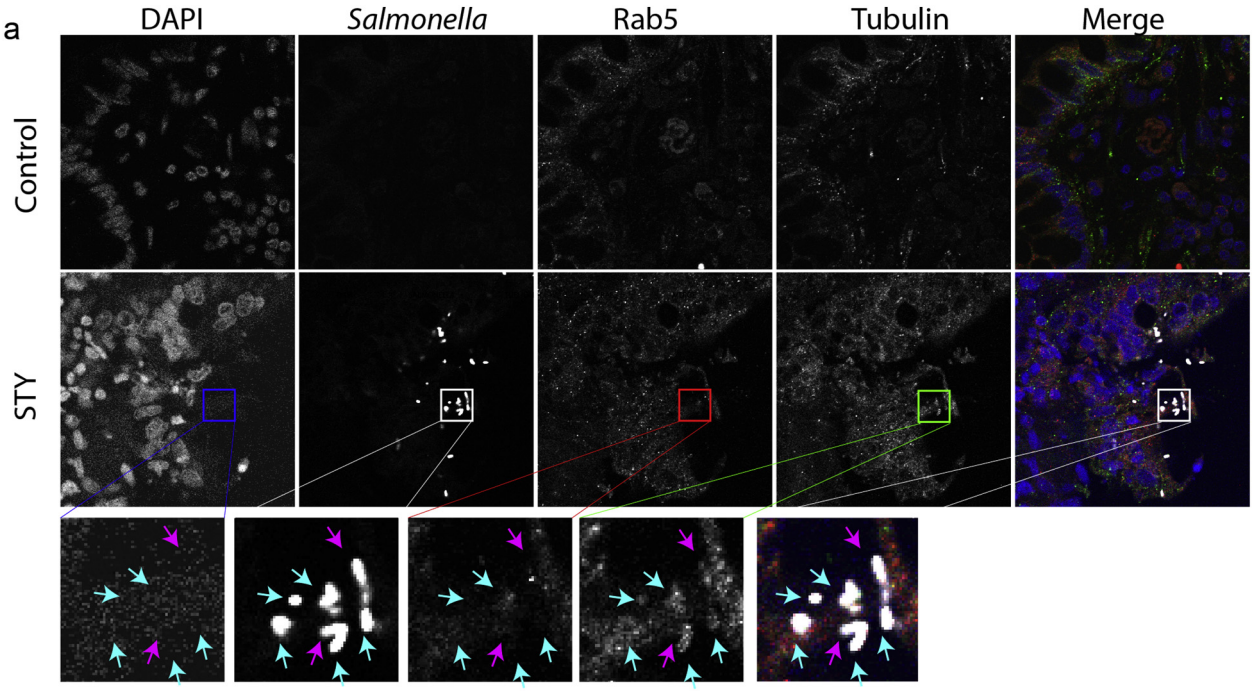
a
DAPI
Salmonella
Rab5
Tubulin
Merge
Control
STY

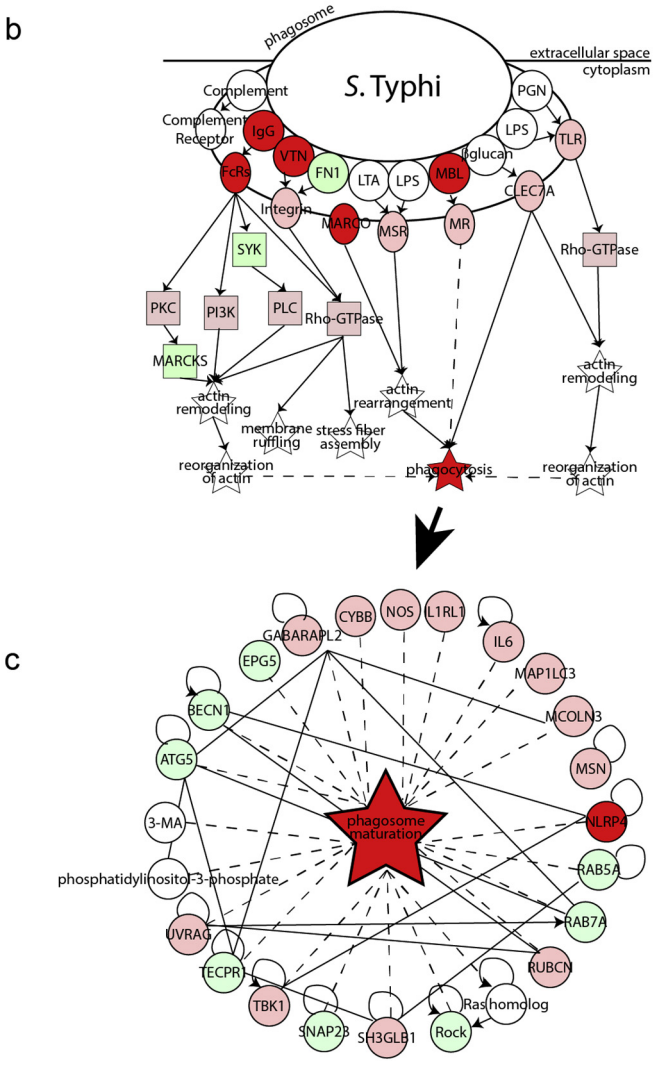
b
phagosome
extracellular space
cytoplasm
S. Typhi
Complement
Complement Receptor
IgG
FcRs
VTN
FN1
LTA
LPS
MBL
β-glucan
PGN
LPS
TLR
CLEC7A
Integrin
MARCO
MSR
MR
SYK
PKC
PI3K
PLC
Rho-GTPase
Rho-GTPase
MARCKS
actin remodeling
actin rearrangement
actin remodeling
membrane ruffling
stress fiber assembly
reorganization of actin
phagocytosis
reorganization of actin
c
CYBB
NOS
IL1RL1
GABARAPL2
IL6
EPG5
MAP1LC3
BECN1
MCOLN3
ATG5
MSN
3-MA
phagosome maturation
NLRP4
phosphatidylinositol-3-phosphate
RAB5A
RAB7A
UVRAG
RUBCN
TECPR1
Ras homolog
TBK1
SNAP23
SH3GLB1
Rock

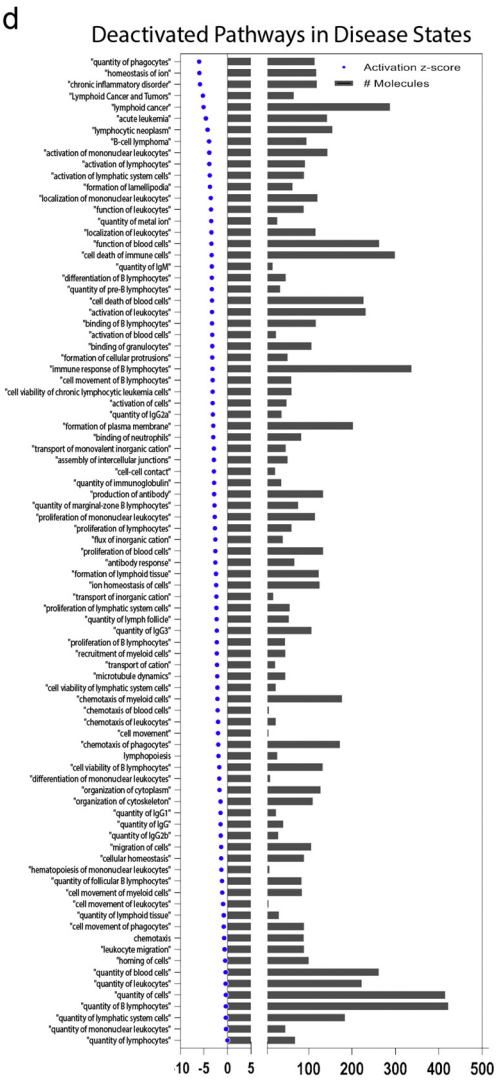
d
Deactivated Pathways in Disease States
Activation z-score
Molecules
"quantity of phagocytes"
"homeostasis of ion"
"chronic inflammatory disorder"
"lymphoid Cancer and Tumors"
"lymphoid cancer"
"acute leukemia"
"lymphocytic neoplasm"
"B-cell lymphoma"
"activation of mononuclear leukocytes"
"activation of lymphocytes"
"activation of lymphatic system cells"
"formation of lamellipodia"
"localization of mononuclear leukocytes"
"function of leukocytes"
"quantity of metal ion"
"localization of leukocytes"
"function of blood cells"
"cell death of immune cells"
"quantity of IgM"
"differentiation of B lymphocytes"
"quantity of pre-B lymphocytes"
"cell death of blood cells"
"activation of leukocytes"
"binding of B lymphocytes"
"activation of blood cells"
"binding of granulocytes"
"formation of cellular protrusions"
"immune response of B lymphocytes"
"cell movement of B lymphocytes"
"cell viability of chronic lymphocytic leukemia cells"
"activation of cells"
"quantity of IgG2a"
"formation of plasma membrane"
"binding of neutrophils"
"transport of monovalent inorganic cation"
"assembly of intercellular junctions"
"cell-cell contact"
"quantity of immunoglobulin"
"production of antibody"
"quantity of marginal-zone B lymphocytes"
"proliferation of mononuclear leukocytes"
"proliferation of lymphocytes"
"flux of inorganic cation"
"proliferation of blood cells"
"antibody response"
"formation of lymphoid tissue"
"ion homeostasis of cells"
"transport of inorganic cation"
"proliferation of lymphatic system cells"
"quantity of lymph follicle"
"quantity of IgG3"
"proliferation of B lymphocytes"
"recruitment of myeloid cells"
"transport of cation"
"microtubule dynamics"
"cell viability of lymphatic system cells"
"chemotaxis of myeloid cells"
"chemotaxis of blood cells"
"chemotaxis of leukocytes"
"cell movement"
"chemotaxis of phagocytes"
lymphopoiesis
"cell viability of B lymphocytes"
"differentiation of mononuclear leukocytes"
"organization of cytoplasm"
"organization of cytoskeleton"
"quantity of IgG1"
"quantity of IgG"
"quantity of IgG2b"
"migration of cells"
"cellular homeostasis"
"hematopoiesis of mononuclear leukocytes"
"quantity of follicular B lymphocytes"
"cell movement of myeloid cells"
"cell movement of leukocytes"
"quantity of lymphoid tissue"
"cell movement of phagocytes"
chemotaxis
"leukocyte migration"
"homing of cells"
"quantity of blood cells"
"quantity of leukocytes"
"quantity of cells"
"quantity of B lymphocytes"
"quantity of lymphatic system cells"
"quantity of mononuclear leukocytes"
"quantity of lymphocytes"
10 -5 0 5
100 200 300 400 500

Table 4
Human-mouse protein homology.

	Gene name	Protein % identity	
		M. musculus	*P. troglodytes*
Genes upregulated upon infection	*GSTM1*	83.90%	97.70%
	C14orf80	69.40%	99.50%
	CRIP1	97.40%	100%[a]
	CCL25	54.30%	98%
	MUC5B	61.60%	91%[a]
	ND3	67.00%	94.80%
	DISP2	76.40%	99.40%
	ND4L	67.30%	99.00%
	ATP8	Human only[b]	92.60%
	ZDHHC11B	Human only[c]	95.20%
	FGFR3	93.40%	95.80%
	EPPK1	75.50%	98.20%
Control genes	*RAB5*	98%	100%
	ACTIN	100%	100%
	RAB7	100%	100%
	TUBULIN	100%	100%
	ZO1	91.10%	99.90%
	MUC2	76%	78%[d]

Please see Supplementary Fig. 5 for additional alignment information.
[a] Predicted protein sequence.
[b] Protein alignment covers 98% with 48% identity - alignment in Supplementary Fig. 5.
[c] Protein alignment covers 78% with 59% identity - alignment in Supplementary Fig. 5.
[d] Protein alignment covers 46% with 78% identity.

Based on the data presented here, only *vexD* is upregulated during early infection of human terminal ileum biopsies. Several genes are downregulated (*phoPQ*, *ssaV)*, while others remain unchanged (*galK*, *ilvD*, *aroC*, *aroD*, *htrA*, *tviA*). These virulence, metabolism and regulatory genes have been considered important targets for initial vaccine candidates [24,41] by creating strains with limited intracellular replication capacity and attenuated virulence. Based on the results of these studies, we propose targeting additional genes specifically upregulated by STY during early infection, namely enzymes and cytoskeletal rearrangement genes. During infection, invading bacteria are efficiently shutting down the host's ability to recognize and respond to infection by manipulating the epithelial cell and blocking recruitment of immune cells to the site of infection. Deletion of genes utilized during early invasion will likely prevent STY from shutting down the host response, thereby permitting infection recognition and restoring the ability to recruit immune cells to the site of infection. Additionally, genes that target RNA degradation may also hold promise as possible targets for vaccine development. By eliminating the bacterium's ability to suppress host gene expression, perhaps we can restore the development of a strong, protective, adaptive immune response.

4.4. An Expanded Model for STY Pathogenesis

As it becomes increasingly clear that our extrapolated data from murine STM studies are insufficient to accurately recapitulate STY pathogenesis in the human host, we have developed a new model that closely resembles the human gut microenvironment to serve as a framework to study STY pathogenesis. Based on our data we propose the following model (Fig. 6): STY invades enterocytes of the terminal ileum through cytoskeletal rearrangement by targeting actin and tubulin networks. Upon entry, the bacteria target Rab proteins to conceal the vesicle from the cellular sorting pathways (a fraction of STY might even escape to the cytosol). During this time, the bacteria block host response transcription by targeting signal transduction pathways normally triggered by bacterial antigens. To prevent recruitment of immune cells to the site of infection, the release of cytokines and chemokines is re-directed via the apical surface toward the lumen of the intestine. By crippling the host recognition of invasion (i.e., by reduced or absent triggering of signal transduction and transcriptional downregulation of antibacterial or cytokine genes) STY exploits a "Trojan horse" strategy to prevent detection. STY is protected from host immune defenses and the bacteria move undetected to the basolateral pole and continue systemic dissemination in the host.

Supplementary data to this article can be found online at https://doi.org/10.1016/j.ebiom.2018.04.005.

Funding

These studies were supported, in part, by NIAID, NIH, DHHS grants R01-AI036525 (to MBS), U19-AI082655 [Cooperative Center on Human Immunology] (to MBS and AF), and U19-AI109776 [Center of Excellence for Translational Research (CETR)] to MBS. The content is solely the responsibility of the authors and does not necessarily represent the official views of the National Institute of Allergy and Infectious Diseases, the National Institutes of Health, NIAID, NIH.

We thank Dana-Farber/Harvard Cancer Center in Boston, MA, for the use of the Specialized Histopathology Core, which provided embedding and sectioning service. Dana-Farber/Harvard Cancer Center is supported in part by an NCI Cancer Center Support Grant # NIH 5 P30 CA06516.

The EM core was supported by NIH/NINDS P30NS045776. Support for the Philly Dake Electron Microscope Facility was provided by NIH 1S10RR023594S10 and by funds from the Dake Family Foundation.

Conflict of Interest

The authors have no conflicts to disclose.

Author Contributions

KPN, SS, RL, LI, CSF, MBS, CF, AF, and MRF were responsible for study design, data generation and data analysis. SP and RL were responsible for donor identification, recruitment and sample collection. DKVK aided in TEM experiments. ZY, CF, KPN and WF were responsible for transcriptomic and related bioinformatics analysis. All authors contributed to manuscript preparation.

Acknowledgements

The authors would like to thank the Diane Capen for her expertise and skill in preparing the samples for TEM analysis. We would also like to thank members of the Fasano, Fiorentino and Faherty laboratories as well as the members of the University of Maryland Cooperative Center on Human Immunology (CCHI) for their thoughtful

Fig. 5. Inside the enterocyte: STY localization and survival. (A) Immunostaining of STY-infected biopsies with cytoskeletal protein tubulin, intracellular early endosome marker Rab5, STY and genomic material (DAPI). STY colocalizes with tubulin during biopsy invasion but exists independent of Rab5. Inset images demonstrating co-localization are marked with a blue arrow; independent STY are marked with a pink arrow. (B) Loss of intracellular early endosome marker indicates masking of cellular localization by STY. RNAseq data predicts inhibition of phagosome formation and maturation; downregulated genes are in red, upregulated genes are in green. (C) Inhibition of phagosome maturation critically impairs antigen harvest and bacterial clearance, which are overarching themes in disease pathways predicted to be downregulated in response to STY infection of terminal ileum biopsies. (D) Predicted deactivated disease states related to the immune response deciphered from downregulation of genes during STY infection. The negative *Z*-score indicates a downregulation of pathways; the number of genes refers to the number of genes downregulated during STY infection that corresponds to the pathway listed. Notable deactivated disease states include quantity of phagocytes, activation of lymphocytes, localization of mononuclear cells, activation of lymphocytes and leukocyte migration.

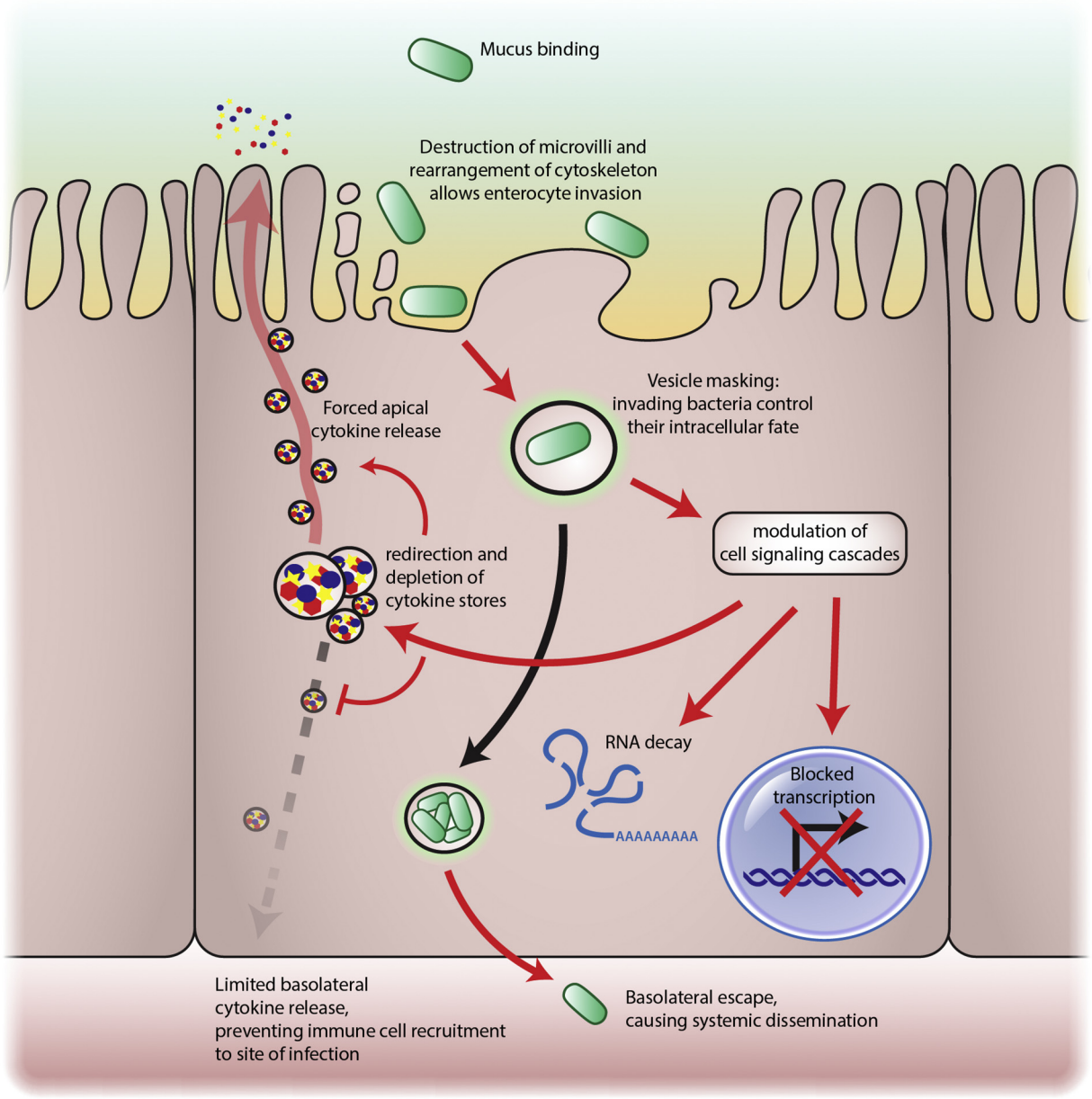

Fig. 6. An expanded model for STY pathogenesis. Taken together, our data demonstrates STY bacteria employ a "Trojan Horse" strategy to invade enterocytes and dismantle the immune response from the intracellular environment. We propose that STY invades enterocytes after rearranging the enterocyte cytoskeleton. Invading bacteria are contained within vesicles that are modified to block vesicular trafficking. The secretion of effector proteins modulates eukaryotic cell signaling cascades and transcription. Cytokine stores are released toward the apical pole to prevent recruitment of immune cells to the site of infection. Finally, STY traverse to the basolateral pole and transition to the systemic phase of disease.

feedback and discussions during the development of the project. A special acknowledgment to Susie Flaherty for her careful editing of the manuscript.

References

[1] Agbor, T.A., Mccormick, B.A., 2011. Salmonella effectors: Important players modulating host cell function during infection. Cell Microbiol:1858–1869 https://doi.org/10.1111/j.1462-5822.2011.01701.x.
[2] Agbor, T.A., Demma, Z.C., Mumy, K.L., Bien, J.D., McCormick, B.A., 2011. The ERM protein, Ezrin, regulates neutrophil transmigration by modulating the apical localization of MRP2 in response to the SipA effector protein during Salmonella typhimurium infection. Cell Microbiol 13 (12):2007–2021 (Blackwell Publishing Ltd). https://doi.org/10.1111/j.1462-5822.2011.01693.x.
[3] Andrews, S., 2018. Babraham bioinformatics - FastQC a quality control tool for high throughput sequence data. (no date). Available at: http://www.bioinformatics.babraham.ac.uk/projects/fastqc/ (accessed 2017).
[4] Anders, S., Huber, W., 2010. Differential expression analysis for sequence count data. Genome Biol 11 (10):R106. https://doi.org/10.1186/gb-2010-11-10-r106.
[5] Anders, S., Pyl, P.T., Huber, W., 2015. HTSeq—a Python framework to work with high-throughput sequencing data. Bioinformatics (Oxford, England) 31 (2):166–169. https://doi.org/10.1093/bioinformatics/btu638.
[6] Antillón, N.M., Warren, J.L., Crawford, F.W., Weinberger, D.M., Kürüm, E., Pak, G.D., et al., 2017. The burden of typhoid fever in low- and middle-income countries: A meta-regression approach. PLoS Negl Trop Dis 11 (2), e0005376.
[7] Arkin, A.P., Stevens, R.L., Cottingham, R.W., Maslov, S., Henry, C.S., Dehal, P., et al., 2016. The DOE systems biology knowledgebase (KBase). bioRxiv Available at:. http://www.biorxiv.org/content/early/2016/12/22/096354, Accessed date: 13 September 2017.
[8] Asmar, R., El Panigrahi, P., Bamford, P., Berti, I., Not, T., Coppa, G.V., et al., 2002. Host-dependent zonulin secretion causes the impairment of the small intestine barrier function after bacterial exposure. Gastroenterology https://doi.org/10.1053/gast.2002.36578.
[9] Azmatullah, A., Qamar, F.N., Thaver, D., Zaidi, A.K., Bhutta, Z., 2015. Systematic review of the global epidemiology, clinical and laboratory profile of enteric fever. J Glob Health 5 (2):20407. https://doi.org/10.7189/jogh.05.020407.
[10] Barthel, M., Hapfelmeier, S., Quintanilla-Martínez, L., Kremer, M., Rohde, M., Hogardt, M., et al., 2003. Pretreatment of mice with streptomycin provides a Salmonella enterica serovar typhimurium colitis model that allows analysis of both pathogen and host. Infect Immun 71 (5):2839–2858. https://doi.org/10.1128/IAI.71.5.2839-2858.2003.
[11] Basnyat, B., Maskey, A.P., Zimmerman, M.D., Murdoch, D.R., 2005. Enteric (typhoid) fever in travelers. Clin Infect Dis 41 (10):1467–1472. https://doi.org/10.1086/497136.

[12] Blackwelder, W.C., Biswas, K., Wu, Y., Kotloff, K.L., Farag, T.H., Nasrin, D., et al., 2012. Statistical methods in the global enteric multicenter study (GEMS). Clin Infect Dis0320 55 (Suppl. 4). https://doi.org/10.1093/cid/cis788.
[13] Birmingham, C.L., Smith, A.C., Bakowski, M.A., Yoshimori, T., Brumell, J.H., 2006. Autophagy controls *Salmonella* infection in response to damage to the *Salmonella* -containing vacuole. J Biol Chem 281 (16):11374–11383. https://doi.org/10.1074/jbc.M509157200.
[14] Campellone, K.G., 2010. Cytoskeleton-modulating effectors of enteropathogenic and enterohaemorrhagic Escherichia coli: Tir, EspFU and actin pedestal assembly. FEBS J 277 (11):2390–2402. https://doi.org/10.1111/j.1742-4658.2010.07653.x.
[15] Choi, J., Shin, D., Kim, M., Park, J., Lim, S., Ryu, S., 2012. LsrR-mediated quorum sensing controls invasiveness of Salmonella typhimurium by regulating SPI-1 and flagella genes. PLoS One 7 (5), e37059 (Edited by N. J. Mantis). https://doi.org/10.1371/journal.pone.0037059.
[16] Corr, S.C., Gahan, C.C.G.M., Hill, C., 2008. M-cells: Origin, morphology and role in mucosal immunity and microbial pathogenesis. FEMS Immunol Med Microbiol 52 (1): 2–12. https://doi.org/10.1111/j.1574-695X.2007.00359.x.
[17] Clark, M.A., Jepson, M.A., 2003. Intestinal M cells and their role in bacterial infection. Int J Med Microbiol 293 (39) Available at:. http://www.urbanfischer.de/journals/ijmm, Accessed date: 12 July 2017.
[18] Deng, L., Song, J., Gao, X., Wang, J., Yu, H., Chen, X., et al., 2014. Host adaptation of a bacterial toxin from the human pathogen salmonella typhi. Cell 159 (6): 1290–1299. https://doi.org/10.1016/j.cell.2014.10.057.
[19] Forbester, J.L., Goulding, D., Vallier, L., Hannan, N., Hale, C., Pickard, D., et al., 2015. 'Interaction of Salmonella enterica Serovar typhimurium with intestinal organoids derived from human induced pluripotent stem cells. Infect Immun 83 (7):2926–2934 (Edited by B. A. McCormick). https://doi.org/10.1128/IAI.00161-15.
[20] Francis, R.S., Berk, R.N., 1974. Typhoid fever. (January). pp. 583–585.
[21] Galán, J.E., 2016. Typhoid toxin provides a window into typhoid fever and the biology of *Salmonella* Typhi. Proc Natl Acad Sci:201606335 https://doi.org/10.1073/pnas.1606335113.
[22] Gart, E.V., Suchodolski, J.S., Welsh, T.H., Alaniz, R.C., Randel, R.D., Lawhon, S.D., 2016. Salmonella typhimurium and multidirectional communication in the gut. Front Microbiol 7:1827. https://doi.org/10.3389/fmicb.2016.01827.
[23] GBD 2013 Mortality and Causes of Death Collaborators, 2015. Global, regional, and national age-sex specific all-cause and cause-specific mortality for 240 causes of death, 1990-2013: A systematic analysis for the global burden of disease study 2013. Lancet 385 (9963):117–171. https://doi.org/10.1016/S0140-6736(14)61682-2.
[24] Galen, J.E., Buskirk, A.D., Tennant, S.M., Pasetti, M.F., 2016. Live attenuated human Salmonella vaccine candidates: Tracking the pathogen in natural infection and stimulation of host immunity. EcoSal Plus 7 (1):1–26. https://doi.org/10.1128/ecosalplus.ESP-0010-2016.
[25] Glotfelty, L.G., Zahs, A., Hodges, K., Shan, K., Alto, N.M., Hecht, G.A., 2014. Enteropathogenic *E. coli* effectors EspG1/G2 disrupt microtubules, contribute to tight junction perturbation and inhibit restoration. Cell Microbiol 16 (12):1767–1783. https://doi.org/10.1111/cmi.12323.
[26] Harding, C.R., Mattheis, C., Mousnier, A., Oates, C.V., Hartland, E.L., Frankel, G., et al., 2013. LtpD is a novel Legionella pneumophila effector that binds phosphatidylinositol 3-phosphate and inositol monophosphatase IMPA1. Infect Immun 81 (11): 4261–4270 (American Society for Microbiology). https://doi.org/10.1128/IAI.01054-13.
[27] Hernandez, L., Hueffer, K., Wenk, M., Galán, J.E., 2004. *Salmonella* modulates vesicular traffic by altering phosphoinositide metabolism. Science 20 (329):946–949. https://doi.org/10.1126/science.1098188.
[28] Homer, C.R., Richmond, A.L., Rebert, N.A., Achkar, J.J., McDonald, C., 2010. ATG16L1 and NOD2 interact in an autophagy-dependent antibacterial pathway implicated in crohn's disease pathogenesis. Gastroenterology 139 (5):1630–1641.e2. https://doi.org/10.1053/j.gastro.2010.07.006.
[29] Höner zu Bentrup, K., Ramamurthy, R., Ott, C.M., Emami, K., Nelman-Gonzalez, M., Wilson, J.W., et al., 2006. Three-dimensional organotypic models of human colonic epithelium to study the early stages of enteric salmonellosis. Microbes Infect 8 (7): 1813–1825. https://doi.org/10.1016/j.micinf.2006.02.020.
[30] Hornick, R.B., Greisman, S.E., Woodward, T.E., DuPont, H.L., Dawkins, A.T., Snyder, M.J., 1970. Typhoid fever: Pathogenesis and immunologic control. N Engl J Med 283 (13):686–691. https://doi.org/10.1056/NEJM197010012831406.
[31] John, J., Van Aart, C.J.C., Grassly, N.C., 2016. The burden of typhoid and paratyphoid in India: Systematic review and meta-analysis. PLoS Negl Trop Dis 10 (4):1–14. https://doi.org/10.1371/journal.pntd.0004616.
[32] Johnson, R., Byrne, A., Berger, C.N., Klemm, E., Crepin, V.F., Dougan, G., et al., 2017 Jan 30. The type III secretion system effector SptP of Salmonella enterica serovar Typhi. J Bacteriol 199 (4). https://doi.org/10.1128/JB.00647-16 (pii: e00647-16).
[33] Keestra-Gounder, A.M., Tsolis, R.M., Bäumler, A.J., 2015. Now you see me, now you don't: The interaction of Salmonella with innate immune receptors. Nat Rev Microbiol 13 (4):206–216 (Nature Publishing Group). https://doi.org/10.1038/nrmicro3428.
[34] Kim, D., Pertea, G., Trapnell, C., Pimentel, H., Kelley, R., Salzberg, S.L., 2013. TopHat2: Accurate alignment of transcriptomes in the presence of insertions, deletions and gene fusions. Genome Biol 14 (4):R36. https://doi.org/10.1186/gb-2013-14-4-r36.
[35] Kaljee, L.M., Pach, A., Garrett, D., Bajracharya, D., Karki, K., Khan, I., 2017. Social and economic burden associated with typhoid fever in Kathmandu and surrounding areas: A qualitative study. J Infect Dis https://doi.org/10.1093/infdis/jix122.
[36] Kolodkin-Gal, I., Engelberg-Kulka, H., 2008. The extracellular death factor: Physiological and genetic factors influencing its production and response in Escherichia coli. J Bacteriol 190 (9):3169–3175. https://doi.org/10.1128/JB.01918-07.
[37] Kolodkin-Gal, I., Hazan, R., Gaathon, A., Carmeli, S., Engelberg-Kulka, H., 2007. A linear pentapeptide is a quorum-sensing factor required for mazEF-mediated cell death in Escherichia coli. Science 318 (5850):652–655. https://doi.org/10.1126/science.1147248.
[38] Kotloff, K.L., Nataro, J.P., Blackwelder, W.C., Nasrin, D., Farag, T.H., Panchalingam, S., et al., 2013. Burden and aetiology of diarrhoeal disease in infants and young children in developing countries (the global enteric multicenter study, GEMS): A prospective, case-control study. Lancet 382 (9888):209–222. https://doi.org/10.1016/S0140-6736(13)60844-2.
[39] Kumar, S., Kolodkin-Gal, I., Vesper, O., Alam, N., Schueler-Furman, O., Moll, I., et al., 2016. Escherichia coli quorum-sensing EDF, a peptide generated by novel multiple distinct mechanisms and regulated by trans-translation. mBio 7 (1), e02034-15. https://doi.org/10.1128/mBio.02034-15.
[40] Langmead, B., Trapnell, C., Pop, M., Salzberg, S.L., 2009. Ultrafast and memory-efficient alignment of short DNA sequences to the human genome. Genome Biol 10 (3):R25. https://doi.org/10.1186/gb-2009-10-3-r25.
[41] Levine, M., 2018. Typhoid fever vaccines. In: Plotkin Stanley, A., Orenstein Walter, A., Paul, A., Edwards Kathryn, M. (Eds.), Vaccines, 7th edn Elsevier, Inc, Philadelphia, PA : pp. 1114–1144 Available at:. https://www-clinicalkey-com.ezp-prod1.hul.harvard.edu/#!/content/book/3-s2.0-B9780323357616000614, Accessed date: 22 August 2017.
[42] Levine, M.M., Kotloff, K.L., Nataro, J.P., Muhsen, K., 2012. The global enteric multicenter study (GEMS): Impetus, rationale, and genesis. Clin Infect Dis 55 (Suppl. 4). https://doi.org/10.1093/cid/cis761.
[43] Lhocine, N., Arena, E.T., Bomme, P., Ubelmann, F., Prévost, M.-C., Robine, S., et al., 2015. Apical invasion of intestinal epithelial cells by Salmonella typhimurium requires villin to remodel the brush border actin cytoskeleton. Cell Host Microbe 17 (2):164–177. https://doi.org/10.1016/j.chom.2014.12.003.
[44] Liu, J., Platts-Mills, J.A., Juma, J., Kabir, F., Nkeze, J., Okoi, C., et al., 2016. Use of quantitative molecular diagnostic methods to identify causes of diarrhoea in children: A reanalysis of the GEMS case-control study. Lancet 388 (10051):1291–1301 (Elsevier Ltd). https://doi.org/10.1016/S0140-6736(16)31529-X.
[45] Lustri, B.C., Sperandio, V., Moreira, C.G., 2017. Bacterial chat: Intestinal metabolites and signals in host-microbiota-pathogen interactions. Infect Immun 85 (12): e00476–17 (Edited by H. L. Andrews-Polymenis). https://doi.org/10.1128/IAI.00476-17.
[46] Mabbott, N.A., Donaldson, D.S., Ohno, H., Williams, I.R., Mahajan, A., 2013. Microfold (M) cells: Important immunosurveillance posts in the intestinal epithelium. Mucosal Immunol 6 (4):666–677 (Nature Publishing Group). https://doi.org/10.1038/mi.2013.30.
[47] Mathura, K.C., Gurubacharya, D.L., Shrestha, A., Pant, S., Basnet, P., Karki, D.B., 2003. Clinical profile of typhoid patients. Kathmandu Univ. Med. J. 1 (2), 135–137.
[48] Matsuhisa, A., Suzuki, N., Noda, T., Shiba, K., 1995. Inositol monophosphatase activity from the *Escherichia coli* suhB gene product. J Bacteriol 177 (1):200–205 Available at:. http://www.ncbi.nlm.nih.gov/pubmed/8002619, Accessed date: 14 September 2017.
[49] Meiring, J.E., Gibani, M., TyVAC Consortium Meeting Group, B, Bentsi-Enchill, A.D., Clemens, J., Darton, T.C., et al., 2017. The typhoid vaccine acceleration consortium (TyVAC): Vaccine effectiveness study designs: Accelerating the introduction of typhoid conjugate vaccines and reducing the global burden of enteric fever. Report from a meeting held on 26-27 October 2016, Oxford, UK. Vaccine 35 (38): 5081–5088. https://doi.org/10.1016/j.vaccine.2017.08.001.
[50] Mogasale, V., Maskery, B., Ochiai, R. L., Lee, J. S., Mogasale, V. V, Ramani, E., Kim, Y. E., Park, J. K., Wierzba, T. F. (2014) Burden of typhoid fever in low-income and middle-income countries: A systematic, literature-based update with risk-factor adjustment, vol. 2. *www.thelancet.com/lancetgh* doi: https://doi.org/10.1016/S2214-109X(14)70301-8.
[51] Mogasale, V.V., Mogasale, V.V., Ramani, E., Lee, J.S., Park, J.Y., Lee, K.S., et al., 2016. 'Revisiting typhoid fever surveillance in low and middle income countries: Lessons from systematic literature review of population-based longitudinal studies. BMC Infect Dis 16:35. https://doi.org/10.1186/s12879-016-1351-3.
[52] Morampudi, V., Graef, F.A., Stahl, M., Dalwadi, U., Conlin, V.S., Huang, T., et al., 2017. Tricellular tight junction protein tricellulin is targeted by the enteropathogenic Escherichia coli effector EspG1, leading to epithelial barrier disruption. Infect Immun 85 (1), e00700-16 (Edited by A. J. Bäumler). https://doi.org/10.1128/IAI.00700-16.
[53] Moreira, C.G., Weinshenker, D., Sperandio, V., 2010. QseC mediates Salmonella enterica serovar typhimurium virulence in vitro and in vivo. Infect Immun 78 (3): 914–926 (American Society for Microbiology). https://doi.org/10.1128/IAI.01038-09.
[54] NCBI, 2017. Identical protein report: Inositol monophosphatase (Escherchia coli str. K-12 substr. MG1655). Available at:. https://www.ncbi.nlm.nih.gov/protein/16130458/?report=ipg, Accessed date: 7 October 2017.
[55] Nesse, L.L., Berg, K., Vestby, L.K., Olsaker, I., Djønne, B., 2011. Salmonella typhimurium invasion of HEp-2 epithelial cells in vitro is increased by N-acylhomoserine lactone quorum sensing signals. Acta Vet Scand 53 (1):44. https://doi.org/10.1186/1751-0147-53-44.
[56] Ngwu, B.A., Agbo, J.A., 2003. Typhoid fever: Clinical diagnosis versus laboratory confirmation. Niger Med J 12 (4), 187–192.
[57] Nickerson, K.P., Homer, C.R., Kessler, S.P., Dixon, L.J., Kabi, A., Gordon, I.O., et al., 2014. The dietary polysaccharide maltodextrin promotes Salmonella survival and mucosal colonization in mice. PLoS One 9 (7). https://doi.org/10.1371/journal.pone.0101789.
[58] Njoroge, J., Sperandio, V., 2012. Enterohemorrhagic escherichia coli virulence regulation by two bacterial adrenergic kinases, QseC and QseE. Infect Immun 80 (2): 688–703. https://doi.org/10.1128/IAI.05921-11.
[59] Orvis, J., Crabtree, J., Galens, K., Gussman, A., Inman, J.M., Lee, E., et al., 2010. Ergatis: A web interface and scalable software system for bioinformatics workflows. Bioinformatics (Oxford, England) 26 (12):1488–1492. https://doi.org/10.1093/bioinformatics/btq167.

[60] Radtke, A.L., Wilson, J.W., Sarker, S., Nickerson, C.A., 2010. Analysis of interactions of Salmonella type three secretion mutants with 3-D intestinal epithelial cells. PLoS One 5 (12):e15750 (Edited by S. Bereswill). https://doi.org/10.1371/journal.pone.0015750.
[61] Raines, S.A., Hodgkinson, M.R., Dowle, A.A., Pryor, P.R., 2017. The Salmonella effector SseJ disrupts microtubule dynamics when ectopically expressed in normal rat kidney cells. PLoS One 12 (2), e0172588 (Edited by E. Cascales). https://doi.org/10.1371/journal.pone.0172588.
[62] Raffatellu, M., Santos, R.L., Chessa, D., Wilson, R.P., Winter, S.E., Rossetti, C.A., et al., 2007. The capsule encoding the viaB locus reduces interleukin-17 expression and mucosal innate responses in the bovine intestinal mucosa during infection with Salmonella enterica serotype Typhi. Infect Immun 75 (9):4342–4350 (American Society for Microbiology). https://doi.org/10.1128/IAI.01571-06.
[63] Raffatellu, M., Wilson, R.P., Winter, S.E., Bäumler, A.J., 2008. Clinical pathogenesis of typhoid fever. J Infect Dev Countries:260–266 https://doi.org/10.3855/jidc.219.
[64] Rauch, I., Deets, K.A., Ji, D.X., von Moltke, J., Tenthorey, J.L., Lee, A.Y., et al., 2017. NAIP-NLRC4 Inflammasomes coordinate intestinal epithelial cell expulsion with eicosanoid and IL-18 release via activation of Caspase-1 and -8. Immunity 46 (4):649–659. https://doi.org/10.1016/j.immuni.2017.03.016.
[65] Rutherford, S.T., Bassler, B.L., 2012 Nov 1. Bacterial quorum sensing: Its role in virulence and possibilities for its control. Cold Spring Harb Perspect Med 2 (11). https://doi.org/10.1101/cshperspect.a012427 (pii: a012427).
[66] Sabbagh, S.C., Forest, C.G., Lepage, C., Leclerc, J.M., Daigle, F., 2010. So similar, yet so different: Uncovering distinctive features in the genomes of Salmonella enterica serovars typhimurium and Typhi. FEMS Microbiol Lett:1–13 https://doi.org/10.1111/j.1574-6968.2010.01904.x.
[67] Scanu, T., Spaapen, R.M., Bakker, J.M., Pratap, C.B., Wu, L., Hofland, I., et al., 2015. Salmonella manipulation of host signaling pathways provokes cellular transformation associated with gallbladder carcinoma. Cell Host Microbe 17 (6):763–774 (Cell Press). https://doi.org/10.1016/J.CHOM.2015.05.002.
[68] Salerno-Goncalves, R., Fasano, A., Sztein, M.B., 2011. Engineering of a multicellular organotypic model of the human intestinal mucosa. Gastroenterology 141 (2): e18–e20. https://doi.org/10.1053/j.gastro.2011.04.062.
[69] Salerno-Goncalves, R., Fasano, A., Sztein, M.B., 2016. Development of a multicellular three-dimensional Organotypic model of the human intestinal mucosa grown under microgravity. J. Vis. Exp. (113) https://doi.org/10.3791/54148.
[70] Shi, D., Li, H., Cheng, A., 2015. Typhoid and paratyphoid fever. Radiology of infectious diseases. vol. 2:pp. 295–303. https://doi.org/10.1007/978-94-017-9876-1_24.
[71] Spanò, S., Liu, X., Galán, J.E., 2011. Proteolytic targeting of Rab29 by an effector protein distinguishes the intracellular compartments of human-adapted and broad-host Salmonella. Proc Natl Acad Sci U S A 108 (45):18418–18423. https://doi.org/10.1073/pnas.1111959108.
[72] Stradal, T.E.B., Costa, S.C.P., 2016. Type III secreted virulence factors manipulating signaling to actin dynamics. Current topics in microbiology and immunology: pp. 175–199 https://doi.org/10.1007/82_2016_35.
[73] Theeya, N., Ta, A., Das, S.S., Mandal, R.S., Chakrabarti, O., Chakrabarti, S., et al., 2015. 'An inducible and secreted eukaryote-like serine/threonine kinase of Salmonella enterica serovar typhi promotes intracellular survival and pathogenesis. Infect Immun 83 (2):522–533 (Edited by B. A. McCormick). https://doi.org/10.1128/IAI.02521-14.
[74] Toapanta, F.R., Bernal, P.J., Fresnay, S., Darton, T.C., Jones, C., Waddington, C.S., et al., 2015. Oral wild-type salmonella typhi challenge induces activation of circulating monocytes and dendritic cells in individuals who develop typhoid disease. PLOS Negl Trop Dis 9 (6), e0003837 (Edited by S. Baker. Public Library of Science). https://doi.org/10.1371/journal.pntd.0003837.
[75] Tran, Q.T., Gomez, G., Khare, S., Lawhon, S.D., Raffatellu, M., Bäumler, A.J., et al., 2010. The Salmonella enterica serotype Typhi Vi capsular antigen is expressed after the bacterium enters the ileal mucosa. Infect Immun 78 (1):527–535. https://doi.org/10.1128/IAI.00972-09.
[76] VanDussen, K.L., Marinshaw, J.M., Shaikh, N., Miyoshi, H., Moon, C., Tarr, P.I., et al., 2015. Development of an enhanced human gastrointestinal epithelial culture system to facilitate patient-based assays. Gut 64 (6):911–920. https://doi.org/10.1136/gutjnl-2013-306651.
[77] Verbeke, F., De Craemer, S., Debunne, N., Janssens, Y., Wynendaele, E., Van de Wiele, C., et al., 2017. Peptides as quorum sensing molecules: Measurement techniques and obtained levels in vitro and in vivo. Front Neurosci 11. https://doi.org/10.3389/fnins.2017.00183.
[78] Virlogeux, I., Waxin, H., Ecobichon, C., Popoff, M.Y., 1995. Role of the viaB locus in synthesis, transport and expression of Salmonella typhi Vi antigen. Microbiology 141 (12), 3039–3047.
[79] Watson, C.H., Edmunds, W.J., 2015. A review of typhoid fever transmission dynamic models and economic evaluations of vaccination. Vaccine 33 (S3):C42–C54 (Elsevier Ltd). https://doi.org/10.1016/j.vaccine.2015.04.013.
[80] Wilson, S.S., Tocchi, A., Holly, M.K., Parks, W.C., Smith, J.G., 2015. A small intestinal organoid model of non-invasive enteric pathogen–epithelial cell interactions. Mucosal Immunol 8 (2):352–361. https://doi.org/10.1038/mi.2014.72.
[81] Winter, S.E., Raffatellu, M., Wilson, P.R., Rüssmann, H., Bäumler, A.J., 2008. The Salmonella enterica serotype Typhi regulator TviA reduces interleukin-8 production in intestinal epithelial cells by repressing flagellin secretion. Cell Microbiol 10 (1): 247–261. https://doi.org/10.1111/j.1462-5822.2007.01037.x.
[82] Winter, S.E., Winter, M.G., Poon, V., Keestra, A.M., Sterzenbach, T., Faber, F., et al., 2014. Salmonella enterica Serovar Typhi conceals the invasion-associated type three secretion system from the innate immune system by gene regulation. PLoS Pathog 10 (7). https://doi.org/10.1371/journal.ppat.1004207.
[83] Yap, K.-P., Gan, H.M., Teh, C.S.J., Chai, L.C., Thong, K.L., 2014. Comparative genomics of closely related Salmonella enterica serovar Typhi strains reveals genome dynamics and the acquisition of novel pathogenic elements. BMC Genomics 15 (1):1007. https://doi.org/10.1186/1471-2164-15-1007.
[84] Zhang, Y.-G., Wu, S., Xia, Y., Sun, J., 2014. *Salmonella* -infected crypt-derived intestinal organoid culture system for host-bacterial interactions. Physiol Rep 2 (9), e12147. https://doi.org/10.14814/phy2.12147.
[85] Zhou, D., Galán, J., 2001. Salmonella entry into host cells: The work in concert of type III secreted effector proteins. Microbes Infect 3 (14–15):1293–1298. https://doi.org/10.1016/S1286-4579(01)01489-7.